NANOFILTRATION MEMBRANES MADE FROM TpPa-1 COVALENT ORGANIC FRAMEWORK NANOFILMS

by

Dalton Sendelbach

A Thesis Submitted in
Partial Fulfillment of the
Requirements for the Degree of

Master of Science
in Engineering

at
The University of Wisconsin-Milwaukee
May 2022

ABSTRACT

NANOFILTRATION MEMBRANES MADE FROM COVALENT ORGANIC FRAMEWORK NANOSHEETS

by

Dalton Sendelbach

The University of Wisconsin-Milwaukee, 2022
Under the Supervision of Professor Xiaoli Ma

Potable water scarcity is a problem growing more severe as water pollution continues to rise and the world population continues to grow. There are many techniques of treating water to remove contaminants and lower salt concentrations to drinkable levels, but there is still a great potential for more sustainable and energy efficient water treatment methods. The use of nanofiltration (NF) membranes appears to be a promising method for treating large quantities of water quickly and without using a lot of energy.

Current nanofiltration membranes used for water treatment have not reached their full potential as they still have lower permeances. Covalent organic frameworks (COFs) are a new type of material with 2D structures and tunable pore sizes currently undergoing a heavy amount of research and development. The use of covalent organic frameworks in nanofiltration membranes could immensely improve their efficiency in water treatment.

In this research work, several techniques and methods were used to produce more efficient NF membranes using COFs (TpPa-1). Several attempts were made to mechanically delaminate and collect COF nanosheets (CONs) from COF powders and to create a thin membrane layer on top of a porous support from the obtained CONs. Grinding COF powders in

a mortar and pestle and liquid sonication were the utilized methods of obtaining CONs but neither method succeeded at consistently producing particle sizes small enough to be considered nanosheets. The other issue with that technique was low adherence of the COFs to the porous support. The COF particles could form a thin layer on top of the support but would wash off when pouring water over the top of it.

Another method of using COFs for NF membrane fabrication was done by synthesizing a COF thin film using interfacial polymerization (IP) and transferring the film to a porous support. The synthesis took place in either a beaker or a vacuum filtration apparatus, with a nylon support at the bottom of the beaker/vacuum filtration apparatus. It took approximately 72 hours to fully complete the polymerization and the thickness of the film could be adjusted by changing the monomer concentrations used. Several thin films were prepared using various monomer concentrations (0.005%, 0.01%, and 0.02%) and using various polymerization times (24hrs, 48hrs, and 72hrs). Upon completion of the polymerization, the liquid layers were removed to combine the thin film to the nylon support. This process usually created several defects in the thin films, as they were very fragile, and the liquid layers were removed by pipetting. Upon removal of the liquid layers, a faster secondary IP was performed on top of the membrane. The secondary IP helped adhere the film to the support and seal up surface defects on the membrane.

The membranes were analyzed using a confocal microscope and tested with Congo Red using vacuum filtration to obtain water permeances and dye rejections. The permeate from the Congo Red was analyzed using UV-Vis spectroscopy to determine the rejection rates of the membranes. The data showed that the membranes prepared using 0.01% monomer concentrations and 24-hour polymerization time produced the thinnest membranes, which had high permeances (above 1,000 $\frac{L}{bar*m^2*hr}$), while still having high rejection rates (above 95%).

The membranes prepared using 0.005% monomer concentrations had the second thinnest films and second highest permeances (above 500$\frac{L}{bar*m^2*hr}$) and the third highest rejection rates (approximately 85%). The average permeance of current commercial NF membranes ranges from about 1-10$\frac{L}{bar*m^2*hr}$ when used for water treatment.

The data from this research suggests that with some fine tuning of monomer concentrations and polymerization times, highly efficient COF thin film membranes can be fabricated for water treatment. Additionally, further work will need to be done to create a more reliable method of attaching the COF thin film to the support without creating defects in the thin film.

TABLE OF CONTENTS

Abstract ii

List of Figures viii

List of Tables xi

List of Abbreviations xii

Acknowledgments xiii

Introduction 1

Membranes 2

Nanofiltration 7

Current NF Membranes 8

NF Membrane R&D 9

Covalent Organic Frameworks 10

Methods of Membrane Synthesis 11

Interfacial Polymerization 13

Nanosheets 16

COF Nanofilms 19

Objective 20

Materials and Methods 20

COF Thin Film 20

Liquid Sonication 21

Secondary IP 22

Thin Film Membranes 23

Results and Discussion 25

COF Membranes Made from CONs 25

Thin Film Membranes 31

0.005% Thin Film 33

0.01% Thin Film 35

0.02% Thin Film 37

24 Hour 0.01% Thin Film 39

48 Hour 0.01% Thin Film 41

Membrane Performance 45

Conclusion 49

Future Work 50

References 52

LIST OF FIGURES

Figure 1: Basic Hollow Fiber Module concept [7-17]…….6

Figure 2: Basic Spiral Wound Module concept [7-17]……6

Figure 3: Basic Plate and Frame Module concept [7-17]……...……6

Figure 4: Types of interfacial polymerization, L_m represents a liquid with a dissolved monomer.[30] *Copyright 2017, Royal Society of Chemistry*…….…...…13

Figure 5: Different classes of interfacial polymerization and their binding mechanisms.[31] *© 2020 Wiley-VCH GmbH*……..…….14

Figure 6: a) Synthesis of DaTp and DaTp-CONs from a cycloaddition reaction with N-hexylmaleimide.[27] *Copyright 2016, Wiley-VCH*……...……18

Figure 7: Vacuum filtration apparatus……..21

Figure 8: a) Laser beam through deionized water. b) Laser beam through CON suspension in deionized water…….....25

Figure 9: Membrane prepared with sonicated TpPa-1 CONs and stored in deionized water…….....……..26

Figure 10: a) Membrane prepared with sonicated TpPa-1 CONs. b) The same membrane after several days of storage in deionized water……26

Figure 11: a) TpPa-1-0.05% and TpPa-1-0.01% thin film after sonication. b) TpPa-1-0.05% and TpPa-1-0.01% thin film after sonication and settling out for several days……...……27

Figure 12: a) CONs on a PES support b) Scattered CONs on PES support after adding water...28

Figure 13: a) CON amine solution on PES support. b) PES support, seconds after adding Tp-hexane solution to the hexane buffer layer. c) Completed TpPa-1 polymerization on PES support……...28

Figure 14: SEM of CON suspension……29

Figure 15: Confocal image of CON suspension at 50X magnification……30

Figure 16: Confocal image of sonicated COF particulate without centrifugation at 50X magnification.....30

Figure 17: FTIR data for TpPa-1 thin film……...……33

Figure 18: 0.005% TpPa-1 thin film on a nylon support before and after performing a secondary IP on the film…….33

Figure 19: 50x Confocal Microscope image of a 0.005% thin film in 3D and 2D……...34

Figure 20: 0.01% TpPa-1 thin film on a nylon support before and after performing a secondary IP on the film…….35

Figure 21: 50x Confocal Microscope image of a 0.01% thin film in 3D and 2D…….36

Figure 22: 0.02% TpPa-1 thin film on a nylon support before and after performing a secondary IP on the film…….……...….37

Figure 23: 50x Confocal Microscope image of a 0.02% thin film in 3D and 2D…….38

Figure 24: 0.01% TpPa-1 thin film synthesized for 24 hours on a nylon support before and after performing a secondary IP on the film……..39

Figure 25: 50x Confocal Microscope image of a 0.01% thin film synthesized for 24 hours in 3D and 2D……40

Figure 26: 0.01% TpPa-1 thin film synthesized for 48 hours on a nylon support before and after performing a secondary IP on the film……..41

Figure 27: 50x Confocal Microscope image of a 0.01% thin film synthesized for 48 hours in 3D and 2D……42

Figure 28: Bar graph of the measured average thicknesses of thin films by monomer concentrations, with root mean square deviations shown as error bars.....43

Figure 29: Bar graph of the measured average thicknesses of thin films by time of polymerization, with root mean square deviations shown as error bars.....44

Figure 30: Measured permeances of membranes in $\frac{L}{bar*m^2*hr}$ by monomer concentration.....45

Figure 31: Measured Congo Red dye rejection rates of membranes by monomer concentration.....46

Figure 32: Measured permeances of membranes in $\frac{L}{bar*m^2*hr}$ by polymerization time.....47

Figure 33: Measured Congo Red dye rejection rates of membranes by polymerization time.....48

LIST OF TABLES

Table 1: Thickness measurements of COF particulate fragment.....31

Table 2: Film thickness results for 50x confocal image of 0.005% thin film……...……35

Table 3: Film thickness results for 50x confocal image of 0.01% thin film……..……...……36

Table 4: Film thickness results for 50x confocal image of 0.02% thin film……...…..38

Table 5: Film thickness results for 50x confocal image of 0.01% thin film synthesized for 24 hours……...40

Table 6: Film thickness results for 50x confocal image of 0.01% thin film synthesized for 48 hours……...……...42

Table 7: Measured membrane permeances and rejection rates by monomer concentration.....47

Table 8: Measured membrane permeances and rejection rates by polymerization time.....49

LIST OF ABBREVIATIONS

COF-Covalent Organic Framework

CON-Covalent Organic Framework Nanosheet

FTIR-Fourier-Transform Infrared Spectroscopy

GO-Graphene Oxide

HFM-Hollow Fiber Module

IP-Interfacial Polymerization

MF-Microfiltration

MMM-Mixed Matrix Membrane

MOF-Metal Organic Framework

NF-Nanofiltration

NIPS-Non-solvent Induced Phase Inversion

Pa- p-Phenylenediamine

PES- polyethersulfone

PFM-Plate and Frame Module

PTSA-p-Toluenesulfonic acid

RO-Reverse Osmosis

SWM-Spiral Wound Module

TFC-Thin Film Composite

TFN-Thin Film Nanocomposite

Tp-1,3,5-triformylphloroglucinol

UF-Ultrafiltration

ACKNOWLEDGEMENTS

I would like to thank Dr. Xiaoli Ma for the extra work and time he spent as my advisor. I would also like to thank Dr. Nidal Abu-Zahra and Dr. Yin Wang for agreeing to be on my examination committee. Lastly, I want to thank my fellow research group members, Zhiqin Qiang, Junwei Wang, Miguel Angel Jaimes, Rahul Sampat Khandge, and Weiling Xia for their assistance and advice.

Introduction

Scarcity of clean, potable water is a problem that is becoming more severe as the world population continues to grow. While not currently a major problem for developed countries, the World Health Organization estimated that approximately 1.7 million people died from complications resulting from the consumption of unsafe drinking water in 2000.[4] The vast majority of these deaths occurred in Africa, and now many large developing countries are also struggling to supply citizens with clean water. China is making great efforts to try and adequately supply a nation of over 1.4 billion people with potable water. Dealing with issues such as industrial and agricultural water contamination as well as vanishing water sources, the water treatments plants in China have struggled to keep up with demands.[5] While there are many different water treatment methods, the research to improve the efficiency of these methods on an industrial scale is becoming more dire. With decreasing freshwater supplies, water desalination could play a major role in helping countries meet their demands.

As early as 1955, Dr. Gilliland wrote a paper with in-depth explanations of the most practical water desalination methods. This paper assessed the likely production capabilities and costs of methods such as electrodialysis, freezing, membrane separation, and several distillation methods, including solar.[6] When this paper was written, there was not a high demand for large-scale water treatment, especially treatment as thorough as water desalination. The processes that were believed to have the most potential for efficiently treating seawater included multieffect and vapor compression distillation, freezing, and electrodialysis.[6] Membrane separation was not an attractive option because they did have the technology to produce a membrane that was permeable to water, but impermeable to salt ions without having extremely low flow-rates. With over 60 years of research and development, membranes have become a more practical and

environmentally sustainable tool for water desalination. Most recently, the discovery of a new material called covalent organic frameworks (COF) has furthered the potential of membrane desalination.

Membranes

Membrane technology is becoming a more prevalent and important tool, used for a more sustainable method of gas and liquid separation. Batteries, fuel cells, distilleries, pharmaceutical and food industries all utilize membrane technology in some way. Membranes mostly rely on pore size to filter material by size exclusion. There are many different membrane designs to facilitate material most efficiently and in a particular manner. These designs revolve around the movement of the feed, permeate, and retentate in the membrane system. The feed is the material that is fed into the membrane system, the permeate is the material that is able to pass through the membrane, and the retentate is the remaining material from the feed that cannot pass through the membrane.[7-17] A measurement of the amount of material able to pass through the membrane with a known surface area in a known timeframe is known as flux (J). Permeance (P), is the same measurement as flux, but also accounts for the pressure across the membrane. The permeability coefficient (P_c) is equal to permeance multiplied by the thickness of the membrane.[7-17]

$$J = \frac{amount\ of\ permeate(m^3, Kg, or\ mol)}{Membrane\ Surface\ Area(m^2) * time(s)}$$

$$P = \frac{J}{pressure(Pa)}$$

$$P_c = P * membrane\ thickness(m)$$

The permeability coefficient is the key indicator for a materials capability as a membrane. In general, materials with higher permeability coefficients are preferred, as they will facilitate material transportation at the highest rate.

There are several other important factors to consider when selecting a membrane material. These factors include fouling, stability, and rejection factor. Fouling is a process that hinders a membrane's performance by gradual buildup of material deposits over the top, or within the membrane pores.[7-17] Several properties affect a material's resistance to fouling when used as membrane. These properties include hydrophilicity, smoothness of the membrane surface, and the surface charge with respect to the charge of solute.[1,18-19] Increased hydrophilicity can reduce membrane fouling when performing an aqueous separation by increasing diffusion through the membrane.[18] Having a smoother membrane surface helps to prevent particulate buildup on the surface of the membrane, preventing pores from being blocked. Having a surface charge that is the same as the solute to be rejected enhances the membrane's antifouling properties by creating a repulsion between the membrane surface and the solute.[1]

Stability plays a crucial role in material selection when considering conditions that will involve strong solvents, extreme pH, and varying temperatures and humidity.[1] It is not only important to ensure the material will be able to withstand the conditions it will be exposed to, but also to know how long it can maintain structural integrity. This gradual breakdown of the membrane's chemical structure is known as membrane physical aging.[7-17] The pace at which membrane physical aging and fouling occur determines how often a membrane will need to be replaced or treated. Physical aging will most likely lead to the replacement of the membrane, but fouling can sometimes be reversed with a backflush. A backflush is simply a reversal of the flow direction through the membrane with the intention of flushing particulate buildup out of the pores.[7-17] A

forward flush could also be performed by simply increasing the feed at a higher rate than standard operating measures. This process helps force particles out of pores, either flushing process can use water, air, or cleaning solutions depending on the type of material.

Rejection factor (R) is a measurement used to show how effectively a membrane removes a particular solute from the feed solution.[7-17] This value is calculated using the equation below:

$$R = 1 - \frac{solute\ concentration\ in\ the\ permeate}{solute\ concentration\ in\ the\ feed}$$

A higher R value correlates with the effective removal of the observed solute. Obtaining higher R values usually requires more time and effort to produce a highly selective membrane, therefore the highest achievable R value is not always the deciding factor for deciding what material to use. Rejection factor is also affected by the processing and design of the membrane.

Membranes can be made of one or many layers, a composite membrane has several layers that differ structurally or chemically.[7-17] Homogenous membranes have a uniform layer with consistent pore sizes, dense membranes have no detectable pores.[7-17] Asymmetric, the most widely used type of membranes, have multiple layers of nonuniform structure.[7-17] The advantage of asymmetric-composite membranes is the ability to combine a thin, yet selective layer, with a more porous and structurally sound layer. This combination yields a highly permeable membrane that is structurally capable of being used in industry.

There are also different mechanisms of introducing feed into the membrane and extracting retentate and permeate. These mechanisms include co-current flow, counter-current flow, cross flow, and dead-end flow.[7-17] Co-current flow works in a pattern where the feed and retentate flow parallel to the membrane and the permeate on the other side flows in the same direction.

Counter-current flows works the same way as co-current except the permeate flows in the opposite direction. Cross flow operates in the same manner with the feed and retentate flowing parallel to the membrane but the permeate flows perpendicular to the membrane. Dead-end flow is the simplest pattern with which the feed and the permeate flow is perpendicular to the membrane and no retentate flow is present.[7-17] These types of flow mechanisms are taken into consideration when processing membrane modules.

Currently, the most utilized membrane modules include spiral wound modules (SWM), hollow fiber modules (HFM), and plate and frame modules (PFM).[20] Spiral-wound membranes consist of a flat sheet membrane spiraled around a core with spacers between membrane layers. The spacers are porous enough to allow the flow of the feed and retentate, while still able to provide structural integrity for the SPM.[21] The core of the SPM consists of a tube with holes in it to allow for permeate to enter. This system utilizes either co-current flow or counter-current flow, depending on which direction the permeate is transported through the core. Hollow-fiber membranes consist of many tubular membranes bundles together, each tube having a diameter of less than one millimeter.[21] The membrane layer can be on the inside, outside, or both sides of the tube. There are two different ways for feed to enter the HFM, though the inside of the tubes, or from the outside. Feed to the inside of the tubes usually allows for the use of greater flowrates, but is more prone to particulate buildup.[21] Feed from the outside of the tubes has limited flowrate potential, but it allows for greater longevity of the membranes as it can be cleaned more thoroughly with a back or forward flush. The PFM consists of a series of non-densely packed flat sheet membranes spaced out enough to allow for high flowrate of the feed. This module is favorable when using solutions with an abundance of suspended particles because

the high flowrate helps prevent buildup on the membrane surfaces by flushing the particles out with the retentate.[21]

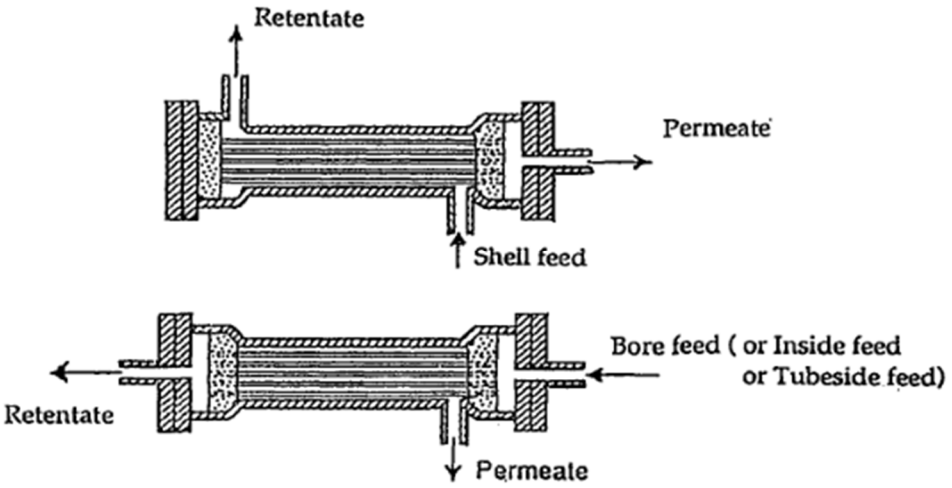

Figure 1: Basic Hollow Fiber Module concept [7-17]

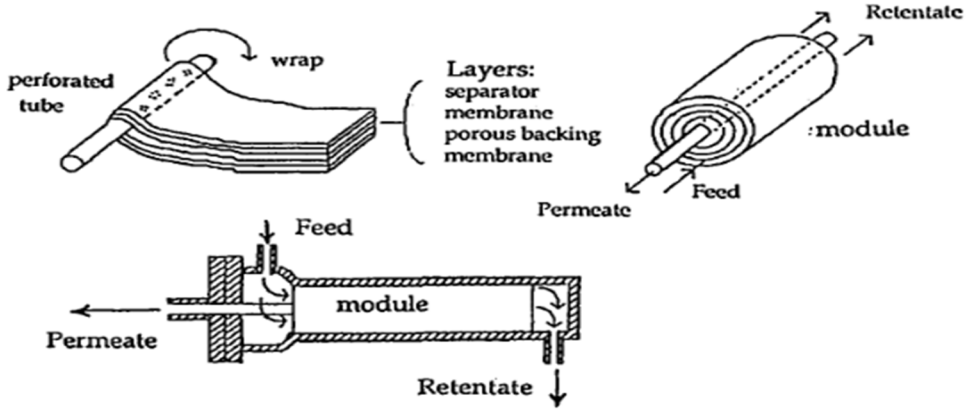

Figure 2: Basic Spiral Wound Module concept [7-17]

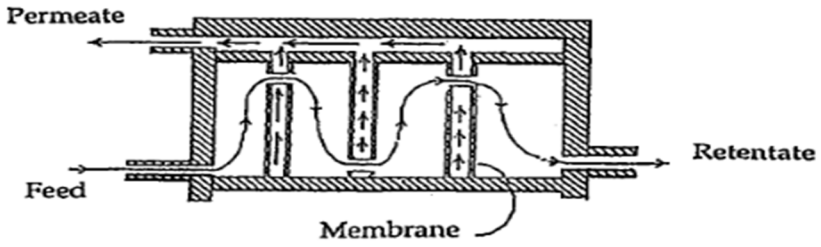

Figure 3: Basic Plate and Frame Module concept [7-17]

Some separations, such as water desalination, require the membrane to have a pore size smaller than 1 nanometer. It is not only challenging to produce a membrane with pores that small, but the membrane must also have high permeability and structural integrity for it to have a practical use in industry. Nanofiltration (NF) and reverse osmosis (RO) membranes can be used to treat and even desalinate water and are currently being produced with well-known amorphous polymers. The SPM and HFM are two particularly utilized types of membranes used for water treatment and desalination. The issues with the current materials being used to make these membranes is a lack of ability to create uniform pore sizes and low porosity.[1]

Nanofiltration

Membranes are classified into different categories based on their pore sizes. These categories include microfiltration (MF) with pore sizes of 0.1-10μm, ultrafiltration (UF) with pore sizes of 0.01-0.1μm, nanofiltration (NF) with pore sizes of 1-10nm, and reverse osmosis (RO) with pore sizes less than 1nm.[22] The type of membrane used for a task depends on the size of the materials being filtered out and how important selectivity is. MF membranes are used to filter out particles and bacteria. UF membranes can filter out proteins, viruses, and larger macromolecules. NF membranes have the potential to filter out ions and small organic compounds and RO membranes can go as far as filtering out minerals, salt and metal ions.[22] Decreasing pore sizes usually leads to an increase in the membrane's selectivity, but lowers the permeance.

The tradeoff between selectivity and permeance is what makes NF membranes particularly attractive for their use in water treatment. UF membranes do not have high enough selectivity to properly treat water and RO membranes do not have a high enough permeance to make them practical at the industrial scale. The main focus for a lot of the research being done on NF

membranes is to produce a thin and structurally sound membrane with uniform pore sizes. For use in water treatment, the charge of the membrane surface is also being researched to help improve permeance and selectivity.[22]

Current NF Membranes

The current NF membranes that are predominantly being used at the industrial scale are commonly made of polyamides, or cellulose-based polymers such as cellulose acetate, cellulose diacetate, and cellulose triacetate.[42] Cellulose-based polymers are convenient to use at the industrial scale because they are cheap to produce and the are resistant to chlorine, which is commonly used to disinfect water. These membranes generally have anisotropic structures with a more densely packed outer layer and a more porous inner layer, though the chemical composition is the same throughout the membrane.[42] The downside of these membranes is a lack of resistance to environments outside of a 4-6 pH range and the permeance and selectivity are inferior in comparison to polyamide membranes.

Polyamides have proven to be far superior in terms of permeance and selectivity, when coated over a porous substrate to form a thin film composite (TFC) membrane. The development of the TFC membrane made it possible to have a thinner, yet highly selective polyamide membrane layer on top of a more structurally robust and porous support layer. A wide variety of supports can be used for TFC membranes depending on the various conditions the membrane will be subjected to. These supports generally include polysulfone, polyimide, polypropylene, etc.[42] The polyamide thin film layer is usually produced on top of the support layer by performing an interfacial polymerization (IP) on the surface of the support.

NF Membrane R&D

Many of the current industrial NF membranes are produced using materials and techniques that were being used over 40 years ago. To improve the efficiency without sacrificing selectivity, much research and development is being conducted to find better materials and methods for NF membrane production. Some newer materials that have great potential to produce efficient NF membranes include graphene oxide (GO), metal organic frameworks (MOFs), and covalent organic frameworks (COFs).

Graphene oxide is a material composed of chemically converted graphene nanosheets, which has proven to be capable of producing membranes with high water permeability and acceptable rejection rates.[42] The challenge is to find a way to produce GO membranes on a larger scale at a reasonable production cost.

The use of MOFs in NF membranes has also gained a significant amount of attention. MOFs are a type of coordination polymers consisting of positively charged metal ions bound together by organic ligands.[43] MOFs can be synthesized to form crystalline and highly porous structures, making them a great candidate for their use in NF membranes. In addition to having high permeability, MOFs have tunability with pore sizes, meaning they can be customly fabricated to precise pore sizes.[43] The main issue with the use of MOFs in membrane technology is there adherence to polymeric supports. The inorganic metal ions in MOFs seem to limit their compatibility and stability on polymeric supports.[43] As polymeric supports are widely used in membrane technology due to their low cost, high permeance, and structural robustness, lack of compatibility is a major drawback for MOFs use in NF membranes.

Stemming off the discovery and research of GO and MOFs was the discovery of COFs. COFs, structurally similar to MOFs, are also crystalline and highly porous.[44] They differ from MOFs in their lack of metal ions, as they consist of organic molecules linked together.[44] The completely organic structure of COFs, in addition to their high porosity and tunability, gives them a significant advantage over MOFs for use in membranes. The advantage of being completely organic is better compatibility with polymeric supports, COFs do not require as much chemical alterations to be compatible with commonly used polymeric supports. While very promising, COFs are very early in research and development and methods of synthesizing a continuous and defect-free COF layer have not yet been developed at an industrial scale.

Covalent Organic Frameworks

Covalent Organic Frameworks (COFs) seem to be a potential solution to the issues with current NF membranes. Yaghi and coworkers first discovered the crystalline porous network structures known as COFs in 2005.[2] COFs are This new type of polymeric material consists of many repeating units of nodes and linkers reacted together to form a porous network.[2] Similar to graphite, COFs consist of many 2D layers packed together by intermolecular forces. The key properties of COFs and their use as membranes include pore size, stability, hydrophilicity/hydrophobicity, and surface charge. Pore size is the most critical property for determining the application of the membrane because membranes largely rely on size exclusion to filter out unwanted materials. Adjusting the pore sizes of COF membranes can be done by altering the size and lengths of the organic linkers and nodes used to construct COFs. Another method is to modify the crystalline network after it has been synthesized by adding large side groups to the inner walls of the COFs, which then decreases the pore size.[3]

Stability is an important factor for membranes to be able to maintain their integrity under various conditions, when used in industry. Stability of COF membranes can be improved by using more stable linkers that have strong covalent bonds and can also be improved by creating more intramolecular hydrogen bonding.[1] Hydrophilicity plays an important role for liquid separations, COFs with greater hydrophilicity have higher flux and less surface fouling than more hydrophobic membranes with similar pore sizes. The main determining factors of hydrophilicity for COFs are the functional groups of the organic linkers.[1] Surface charge is a property that has not yet received a large amount of research. The research that has been done, shows that when COFs have functional groups with the same charge as the solute, there seems to be improved rejection rates and better antifouling properties. This is a result of the electrostatic repulsion between the functional groups on the membrane surface and the solute.[1] Much research is being done to utilize the great potential for COFs in many different applications. To make use of COFs for improving current NF membranes, much research still needs to be done on the methods of synthesis and how to process the COFs into membranes with industrial sized output. While currently in early years of research and development, COFs appear to have the potential to produce low density, more precise, and highly efficient membranes.

Methods of Membrane Synthesis

There are several methods used to synthesize COF membranes including blending, solvothermal, and layer-by-layer stacking. In blending, COFs are combined with traditional polymer membranes. The types of membranes created from blending include mixed matrix membranes (MMMs) or thin film nanocomposites (TFN). A process called non-solvent induced phase inversion (NIPS) is used to create MMMs. This is done by creating a homogenous solution of COFs and polymers in an organic solvent and then removing the solvents to obtain a MMM.[1]

Interfacial polymerization (IP) is the process used to produce TFN . IP is performed by combining an aqueous amine solution with an organic solution containing a different monomer, creating a thin film of COF at the interface of the two liquids. The created thin film can be synthesized directly on the surface of a polymer support, or it can be transplanted on top of a support after its creation to produce a TFN.[23] The main difficulty is producing a defect-free COF layer that maintains structural integrity while managing to adhere to the polymer support.

Solvothermal is a method designed by refining earlier synthesis methods for COFs, which can be used to make free standing COF films and COF based composite membranes.[1] In this process, different monomers are combined to allow for the formation of COFs and are baked for a period of 12-72 hours.[24] The result is a free standing COF with mechanical stability that can maintain integrity in water, organic solvents, and some acids.[24] The drawback to his method is the use of larger quantities of COF precursors, the thickness of the membrane needed to maintain mechanical stability, and the long processing time attributed to the baking step.

The methods mentioned above are all examples of bottom-up strategies for membrane production because each step of the COF synthesis is also part of the membrane fabrication. Layer-by-layer stacking is an example of a top-down strategy because bulk COF powders are first prepared, before being processed and modified to produce a membrane. Layer-by-layer stacking is a method of stacking COF nanosheets (CONs) onto a support, forming multiple layers.[1,25] Bulk COF powders consist of many sheets stuck together through van der Waals or hydrogen bonding. These forces are also known as π-π interactions, which can be broken to obtain CONs of only a few layers, without damaging the bonding within each sheet.[25] Once obtained, CONs can be used to produce membranes by either filtering a CON suspension through a porous support, or by dipping a support into a the suspension.[1]

Interfacial Polymerization

Interfacial Polymerization (IP) is a type of reaction to combine monomers and form longer chains at the interface of two immiscible phases.[30] These interfaces can include liquid-liquid, liquid-solid, and liquid-gas/air.[30] The surface area conjoining the two phases is the interface where the polymerization will take place. The monomer undergoing the polymerization will need to be dissolved in one of the liquids involved in the IP. In many liquid-liquid polymerizations, the two phases will each contain a different monomer, which will polymerize at the interface. Figure 5 visualizes the different types of IP but fails to include liquid-gas and the possibility of a porous solid containing a monomer of its own.

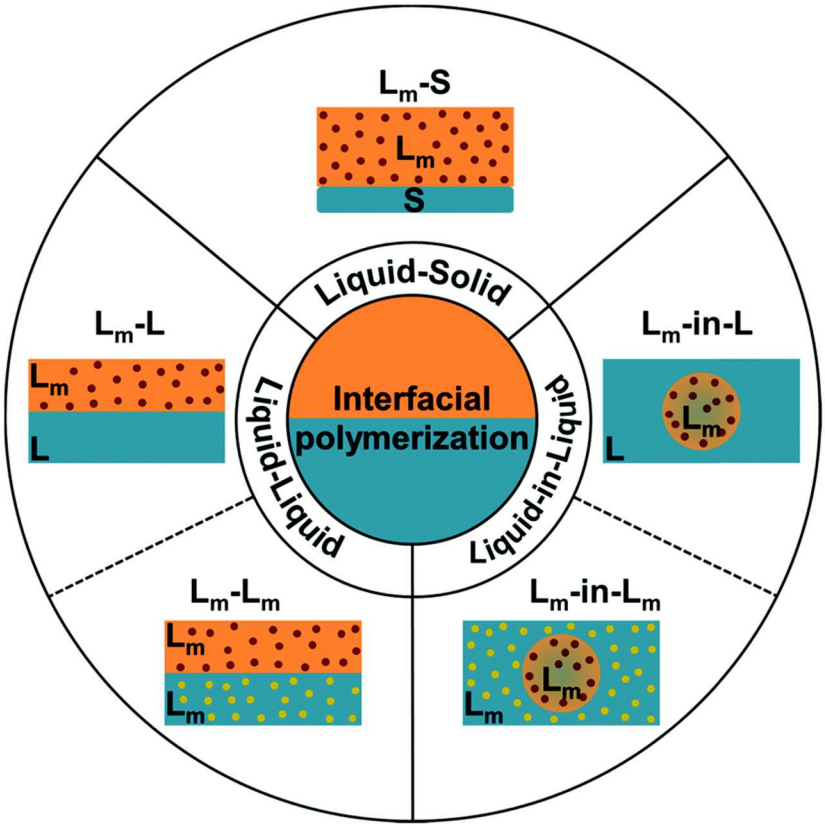

Figure 4: Types of interfacial polymerization, L_m represents a liquid with a dissolved monomer.[30] Copyright 2017, Royal Society of Chemistry

In a usual IP, a thin film is rapidly produced at the interface as the monomers react.[31] As the polymerization continues and the film thickens, the reaction begins to slow until the layer is too thick for monomers to diffuse across.[31] Adjusting the polymerization time allows for some control over the thickness of the film, though it will reach a maximum thickness if allowed enough time. While time is an important factor to consider, many other chemical properties involved with the polymerization, especially monomer concentrations will affect the final thickness and morphology of the thin film.[32]

In addition to the different phases involved in IP, further distinctions can be made based on the types of reactions that occur during the polymerization. These distinct types of reactions can be categorized as polycondensation, polyaddition, supramolecular polymerization, oxidative polymerization, or polycoordination.[31]

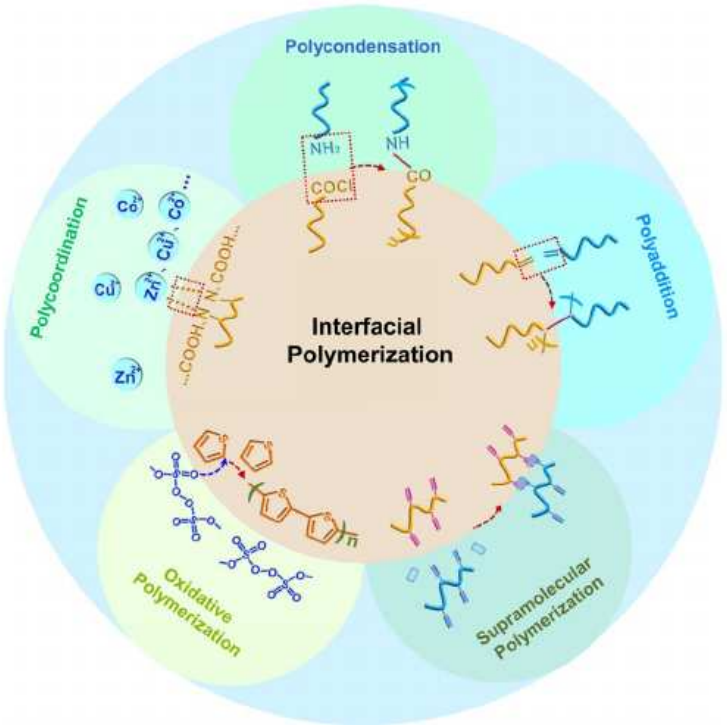

Figure 5: Different classes of interfacial polymerization and their binding mechanisms.[31]

Interfacial polycondensation is the earliest discovered type of IP.[31] It is distinct because of its use of multifunctional monomers that undergo a condensation reaction, producing polymer chains and some other small molecule byproducts.[33] Common polymers such as polyamide, polyimides, polyesters, and polyurethanes are all produced using interfacial polycondensation.[31]

Interfacial polyaddition is a process of combining monomers without producing byproducts. Monomers are able to combine through various mechanisms including radical, anionic, cationic, and ring-opening polymerizations.[31] All of these polymerization mechanisms fall within the polyaddition category. Polyaddition is mostly used to produce polymers such as polyurethanes and polyurea through a water-oil interface.[31] This type of polymerization is usually done using oil and water as the two liquid phases. Commonly, the polymerization occurs is a liquid-in-liquid meaning drops of oil are suspended in water, as opposed to there being one large surface interface between the two liquids. This is also referred to as emulsion polymerization and it usually used to produce hollow capsules.[31]

Interfacial oxidative polymerization is a process that uses an oxidizing agent to combine monomers through oxidative coupling.[31] Typically this type of IP uses an oxidant dissolved in an aqueous solution and a monomer dissolved in an organic solvent and produces a conducting polymer film or nanofiber.[31] Some of the more popular conducting polymers created using interfacial oxidative polymerization include polyaniline, polypyrrole, and polythiophene.[34] Conducting polymers are particularly attractive in the field of polymer science because of their electrical, magnetic, and optical properties, which resemble that of a metal, while having the mechanical properties of a polymer.[35]

Interfacial supramolecular polymerization combines monomers using reversible, noncovalent bonds such as hydrogen bonding, metal coordination, and van der Waals forces.[36] Still early in

the research and development phase, production of supramolecular polymers is still a challenge, but IP seems to be a promising method of reliable production.[31] Supramolecular polymers have gained interest because of the unique properties they posses such as reversibility of bonding and ability to self-repair, which could be very promising in their use in biomaterials and electronics.[31,37-39]

Interfacial polycoordination is a process that uses metal cations and organic ligands as precursors, which are combined through covalent or coordinate bonds, with secondary weaker bonds as well.[31,40] The resulting coordinate polymers created are composed of metal-organic linkers, with a possibility of being one-, two-, or three-dimensional.[31] Three-dimensional coordinate polymers tend be bonded more covalently and are therefore more stable, these polymers are referred to as metal-organic frameworks (MOFs).[41] The highly discovery of the highly porous MOFs helped pave the way for the discovery of the two-dimensional COFs.

COFs can be polymerized in multiple ways, but IP has made it possible to easily produce continuous COF films. Currently there are two types of IP that can be used to produce COFs, which are polyaddition and polycondensation.[31] The potential that COFs show for their use as membranes has made IP a particularly attractive method of COF production, and has greatly increased the demand for research and development.

Nanosheets

Nanosheets are 2D chemical structures that can generally range from 1 to 100nm thick.[45] The first successful creation of nanosheets was single layered carbon graphene, which sparked a vast amount of research on 2D nanomaterials.[45] Many fields of technology have a great potential for improvement with the use of nanosheets such as, solar cells, biomedicine, batteries, sensors, and

membranes.[45] The structures of COFs are quite similar to the structure of graphite as they consist of many layers of 2D sheets bound together by π-π bonds. This similarity has given COFs a significant amount of attention for the delamination of bulk COFs to produce COF nanosheets (CONs).

CONs are obtained by the exfoliation of bulk COF powders using one of several techniques.[1] These techniques include solvent-assisted, chemical, mechanical, and self-exfoliation.

Solvent-assisted exfoliation is performed by sonicating the COF powder in a solvent with a similar surface energy. Sonication speeds up the intercalation of the solvent into the COF powders to break the forces holding the layers together and the use of a suitable solvent will keep them from recombining.[25] It is crucial to use a solvent that is not strong enough to break the covalent bonds within the CONs.

Mechanical exfoliation is simply a process of grinding down COF powders to break the forces holding the COF layers together and form CONs. The first successful attempt to produce CONs using mechanical exfoliation used a mortar and pestle and a few drops of methanol to grind up the COF powders.[26] The ground up powder was then suspended in water and centrifuged to the point where the bulk COF powders formed a pellet at the bottom of the tube and the CONs remained suspended in the water. Ball milling is another method of mechanical exfoliation where powders are loaded into a container and spun at controlled frequencies. Also in the container are balls made of hard metal, which grind down the powders as the container spins.[25] The CONs can then be extracted from the ground down powder the same as with the mortar and pestle process.

Chemical exfoliation is performed with the use of a cycloaddition reaction to disrupt the forces keeping the layers together.[27] The cycloaddition reaction introduces a molecule that bonds to the COF layers in a way that hinders van der Waals forces and hydrogen bonding. The exfoliated CONs can then be dissolved in a volatile organic solvent and poured over water, once the solvent evaporates, the CONs will remain on top of the water as a free-standing thin film.[27]

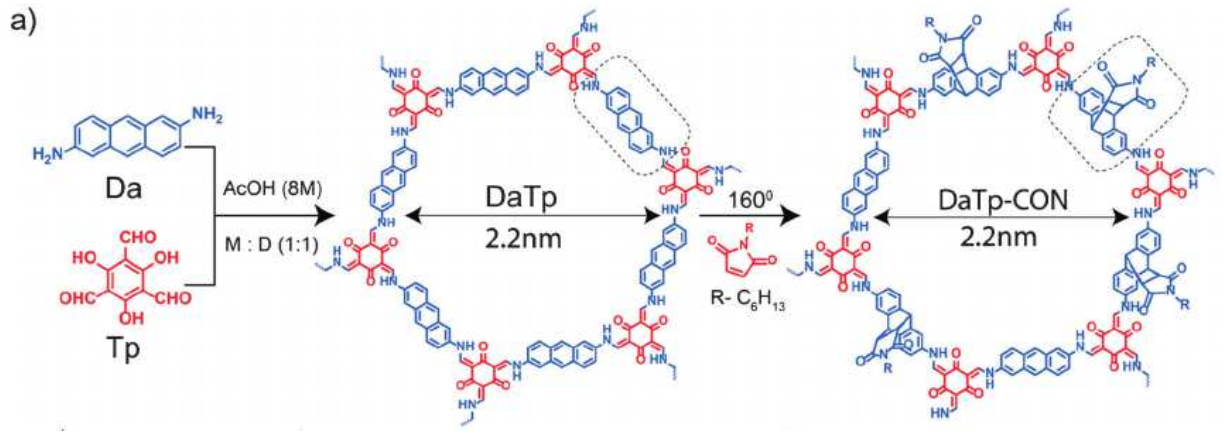

Figure 6: a) Synthesis of DaTp and DaTp-CONs from a cycloaddition reaction with N-hexylmaleimide.[27] Copyright 2016, Wiley-VCH

The self-exfoliation method is clever process of preventing COF layers from being forced together as they are synthesized, eliminating the need for external forces. One of the ways to synthesize self-exfoliating COFs, is to use precursors with bulky molecular groups that will sterically hinder the layers from coming together.[28] The bulky molecular groups will keep distance between COF layers and prevent the forces of van der Waals and hydrogen bonding. Another method is to use ionic precursors to synthesize COFs, resulting in COF layers with similar charges that will repulse each other.[29] Both methods have succeeded in producing CONs of only a few layers thick.

COF Nanofilms

COF nanofilms are continuous COF layers that are less than 1 μm thick. The use of COF nanofilms to produce membranes utilizes the high permeability and selectivity of COF nanosheets, while having more control over the thickness of selective layers and without the risk of any dispersion issues. The challenge with using COF nanofilms to produce membranes is transferring a continuous, defect free film to a porous substrate without damaging the film in the process.

Several different methods have been used to employ COF nanofilms as selective membrane layers. One method used solvothermal polymerization to produce a COF nanofilm on a silicon substrate and then coated the nanofilm with a porous copolymer layer, which acted as a protective layer. The added protective layer made it possible to transfer the COF nanofilm to a porous substrate, where it remained sandwiched between the two porous layers.[45] This method was successful in protecting the COF nanofilm, but the resulting membrane had an additional polymer layer susceptible to fouling and potentially providing other issues.

A simpler method utilized IP to produce a COF nanofilm, which was then directly transferred to a porous substrate. The direct transfer of the COF nanofilm to the porous substrate was made possible with the use of a Langmuir-Blodgett trough.[46] The use of IP inside the Langmuir-Blodgett trough with a porous support at the bottom of the trough made it possible to slowly drain the liquid from the IP, and lower the COF nanofilm to the substrate. After draining all the liquid used in the IP, the bottom of the trough would contain the porous support with a continuous COF nanofilm attached to the surface.[46]

Objective

The goal of this research is to fabricate more efficient NF membranes with the use of TpPa-1 COF. Membranes were prepared using several methods and techniques to determine how to successfully utilize the high permeability and selectivity of COFs. The first method tested involved the delamination of TpPa-1 thin films by sonication, with the intent of obtaining CONs. The obtained CONs were then used to coat a porous support, with the intent of creating a selective yet highly permeable layer.

Another method utilized a fully intact TpPa-1 thin film to coat a porous support. This was accomplished by using IP in a beaker, with a porous support beneath the interface of the two liquids. After formation of the thin film, the liquids could be carefully removed to attach the thin film to the support. Both methods received a rapid secondary IP after coating the support with the selective layer as a way of improving the adherence and sealing any defects. The thin film method was further explored by adjusting the monomer concentrations used in the IP and by varying the polymerization times. These changes were analyzed by their effect on film thickness, permeance, and rejection rates of Cong Red dye.

Materials and Methods

COF Thin Film

Two different concentrations of TpPa-1 thin films were created using IP. To synthesize TpPa-1-0.05% thin film, 31.4 mg of 1,3,5-triformylphloroglucinol (Tp) was dissolved in 40 mL dichloromethane in a 100 mL beaker. 20 ml pure water was added on top of the Tp-dichloromethane solution as the spacer solution. 24.3 mg of Pa and 77.4 mg p-Toluenesulfonic

acid (PTSA) were dissolved in 20 mL water. Slowly, the Pa-PTSA-water solution was added on top of the spacer solution. The system was left undisturbed and at room temperature for 72 hours. After the thin film formed on the liquid interface, the solutions were removed using pipettes. The thin film remained, stuck to the bottom surface of the beaker. The thin film was then washed with ethanol and methanol and was then stored in methanol. The steps in this SOP were then duplicated to synthesize TpPa-1-0.01% thin film using one fifth the amounts of Tp, Pa, and PTSA.

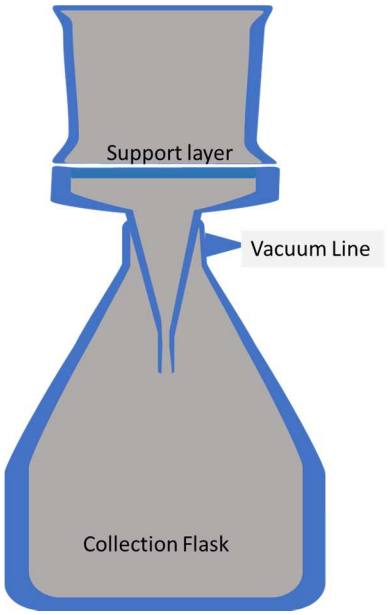

Figure 7: Vacuum filtration apparatus

Liquid Sonication

To obtain CONs the COF thin films were then exfoliated using liquid sonication for several hours while suspended in deionized water. The CON suspensions were then centrifuged and allowed time for the particulate to settle to the bottom of the test tubes. Once settled, the supernatant was collected from the test tubes with the assumption that CONs would be

suspended in the water. The supernatant could then be poured over the top of a PES support affixed inside a vacuum filtration apparatus (shown in figure 7) under low vacuum pressure. This created a thin coating of CONs on top of the support.

Secondary IP

As a method of sealing any defects and aiding with adherence to the support, a secondary IP was performed on top of the CONs layer. First, a Tp-hexane solution was created by dissolving 1.75 mg of Tp in 10 mL of hexane in a glass vial. The vial was then sonicated for a few minutes to thoroughly break up the Tp powder and allow it to dissolve. Then an amine solution was prepared using 10 mL of a CON-water suspension, 200 mg of Pa, and 100 μL of acetic acid. The amine solution was sonicated for several minutes.

A PES support was affixed to the vacuum filtration apparatus and the 10 mL of amine solution was slowly pipetted on top of the support. A 10 mL buffer layer of pure hexane was added on top of the amine solution and allowed to settle out for several minutes. Vacuum pressure was slowly turned on to pull the amine solution through the support while the hexane remained on top of the support, unable to pass through the pores of the support. The hexane layer on top of the support acted as a buffer to prevent disruption of the thin CON layer on the PES surface. The Tp-hexane solution was then slowly pipetted on top of the hexane buffer layer. The polymerization was allowed to go for several minutes before the hexane was carefully pipetted from the apparatus.

The membrane was then removed from the apparatus placed in beaker with pure hexane for several minutes to wash off any unused reactants. To further was the membrane, it was then

placed in a beaker with methanol and allowed to sit for 15-20 minutes. After being removed from the methanol, the membrane was rinsed with deionized water, and stored in a petri dish with deionized water.

To use a consistent quantity of CONs, a bulk stock suspension of TpPa-1-0.01% thin film CONs was prepared. The stock suspension contained the supernatant of numerous liquid sonicated TpPa-1-0.01% suspensions and was used for all membrane fabrications.

Thin Film Membranes

Thin film membranes were fabricated by creating a TpPa-1 thin films under various conditions using the same IP methods as before, but with a nylon support submerged at the bottom of the Tp-dichloromethane layer. The polymerization was performed in 150mL beakers and in the vacuum filtration apparatus. The standard polymerization conditions for the thin films were using 0.01% concentrations of the monomers in each solution and allowed 72 hours to grow at room temperature, with a secondary IP performed on each. Other concentrations of TpPa-1 thin films tested were 0.02%, and 0.005%, both allowed 72 hours of growth time. Time of polymerization was another tested condition; 0.01% thin films were allowed to grow for 24 hours and 48 hours before being tested. Under each of these conditions, all membranes received a secondary IP on the finished membrane before testing except for the membranes prepared in the vacuum filtration apparatus, which were rinsed with water and tested immediately.

When using the 150mL beaker, the nylon support would float in the dichloromethane layer, but would stay below the film at the interface. At the end of the polymerization, a disposable pipette was used to remove the liquid layers from the beaker. The bottom Tp-dichloromethane layers

was removed first by piercing the thin film at the edge, and slowly pipetting until the thin film was on top of the support (removing the top Pa-water layer first would lead to the thin film contracting and coming apart after the last of the water is removed). Then the Pa-water solution was removed as carefully as possible to avoid disturbance of the thin film. To remove the remaining reactants, the thin film was then rinsed several times by slowly pipetting deionized water on top of the membrane and slowly pipetting it off. As a means of keeping the thin film adhered to the nylon support, a secondary IP was performed on top of the membrane. Using the same concentrations as done with the previous secondary IPs (without the use of CONs), the Pa-water solution was pipetted on to the membrane and pipetted off within 30-40 seconds. Then the Tp-hexane solution was pipetted on to the membrane and pipetted off within 30-40 seconds. The membrane was then rinsed with pure hexane and then deionized water using the same pipetting methods as before. The membrane could then be stored in deionized water or tested immediately.

When using the vacuum filtration apparatus, a nylon support was placed over the mesh screen and wetted with deionized water to keep it properly seated, and to help prevent dichloromethane from leaking through the support. At the end of the polymerization, vacuum pressure was slowly turned on to pull the Tp-dichloromethane and Pa-water layer through the support. With the thin film affixed to the support and the vacuum pressure set to around 20 kPa, deionized water was slowly pipetted over the membrane to rinse any remaining reactants through the support. The film could then be used for testing, unless preforming a secondary IP. If preforming a secondary IP, it was done by pipetting Pa-water solution on top of the membrane and using vacuum pressure to pull the solution through the membrane in approximately 30 seconds. The Tp-hexane solution was then pipetted on top of the membrane and pipetted off in 30-40 seconds. The

membrane was rinsed by pipetting pure hexane to the top of the membrane and pipetting it off. Deionized water was then pulled through the membrane under vacuum pressure to complete the rinse. The membrane was then stored in deionized water or tested immediately.

Results and Discussion

COF Membranes Made from CONs

a) 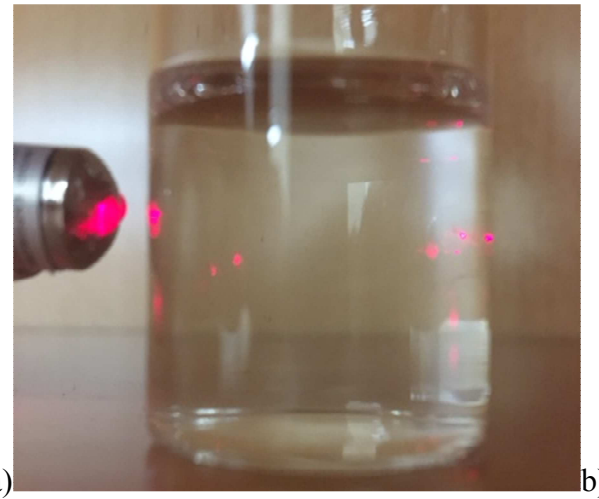 b) 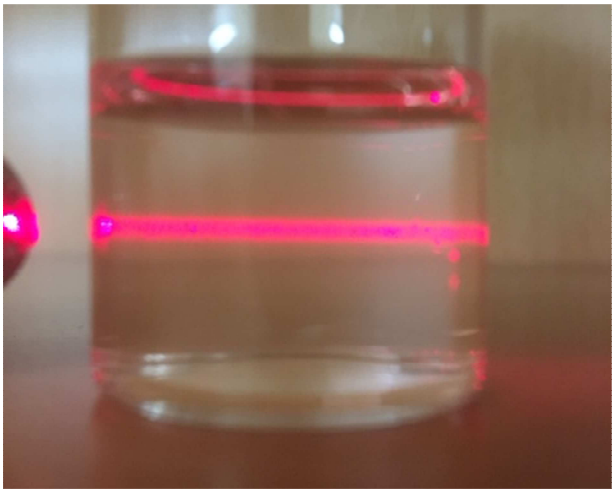

Figure 8: a) Laser beam through deionized water. b) Laser beam through CON suspension in deionized water.

It was evident that COF thin films could be broken down into much smaller particles and possibly CONs by liquid sonication of the films. Figure 8 b) shows a laser beam passing through the supernatant of a mixture of COF powders that had been sonicated for several hours and allowed to settle out for several days in an upright test tube. A phenomenon known as the Tyndall effect is displayed in the figure, as the laser beam is visible due to the suspended particles in the water. Several attempts were made to produce membranes from CON suspensions by pouring them onto PES supports affixed in a vacuum apparatus.

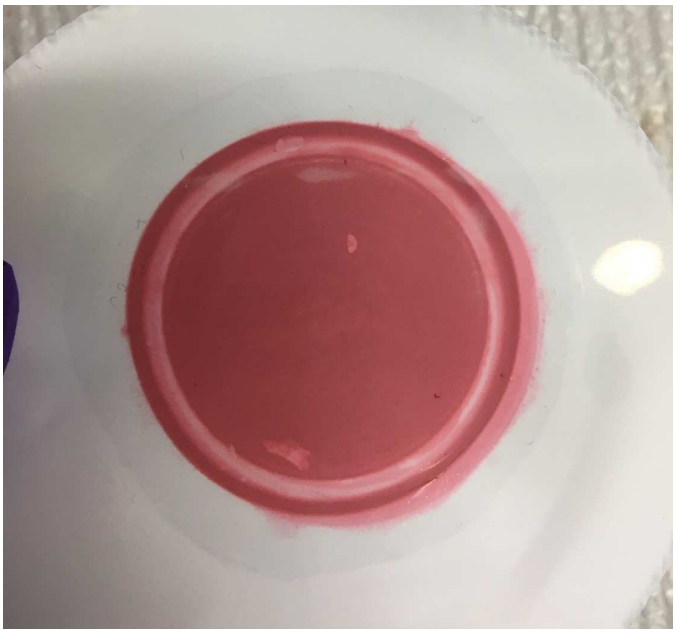

Figure 9: Membrane prepared with sonicated TpPa-1 CONs and stored in deionized water

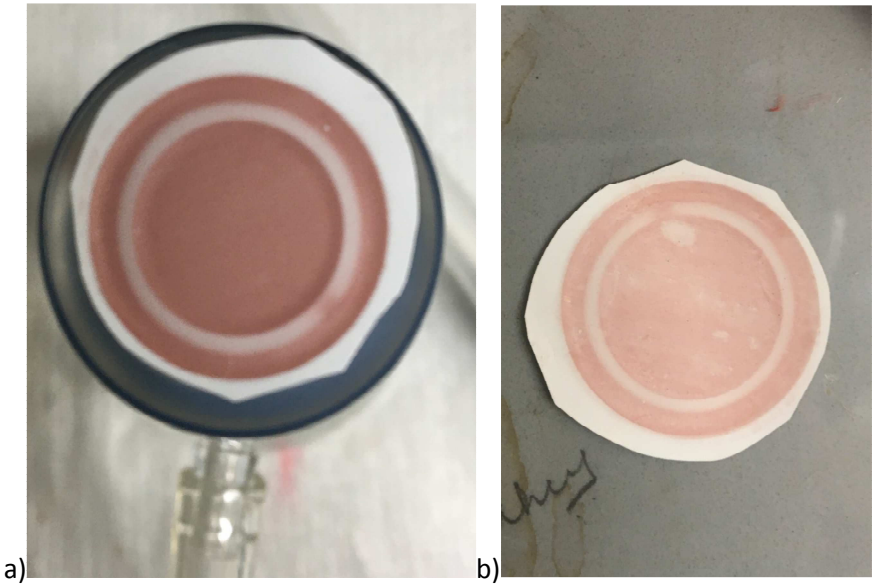

Figure 10: a) Membrane prepared with sonicated TpPa-1 CONs. b) The same membrane after several days of storage in deionized water.

Figures 9 and 10a show evidence of a CONs layer forming on top of the support after pouring the supernatant of a CON suspension (shown in in figure 11) on top of it. The supernatant of the

CONs suspension appeared to be clear (seen in figure 11b), but approximately 20mL of the suspension was able to coat the support with a layer of CONs.

a) 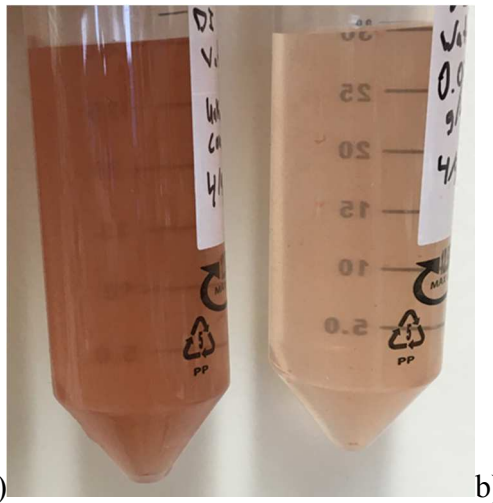 b) 

Figure 11: a) TpPa-1-0.05% and TpPa-1-0.01% thin film after sonication. b) TpPa-1-0.05% and TpPa-1-0.01% thin film after sonication and settling out for several days.

The CONs displayed a clear lack of adherence to the PES support, placing the membranes in water after fabrication led to CONs gradually floating off the supports. Figure 10b displays the lack of adherence of the CONs to the PES support, the CON layer is clearly a lighter shade of red and has some bare spots on it not seen in figure 10a. Figure 12 shows how pouring water on the membrane disrupts the CON layer. This phenomenon made it impossible to test the CON membranes even immediately after fabrication, because the testing itself would disrupt the membrane layer.

a) 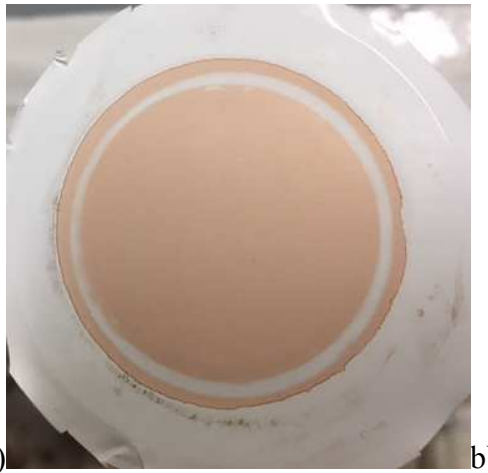 b) 

Figure 12: a) CONs on a PES support b) Scattered CONs on PES support after adding water

Secondary IP (shown in figure 13) was used in an attempt to lock the CONs in place and prevent them from scattering on the PES support, while also sealing any potential defects. The secondary IP succeeded at polymerizing a TpPa-1 layer on the support surface. While successfully creating a TpPa-1 layer on the surface, this method failed to lock the CONs in place. The addition of the Tp-hexane solution to the top of the CON layer caused the CONs to disperse faster than the secondary IP could lock them into place.

a)  b)  c) 

Figure 13: a) CON amine solution on PES support. b) PES support, seconds after adding Tp-hexane solution to the hexane buffer layer. c) Completed TpPa-1 polymerization on PES support.

The CON suspensions were further characterized using a scanning electron microscope (SEM) and a confocal microscope. Samples were prepared by drying a few milliliters of CON suspension on a glass slide for the microscope and a silicon wafer for SEM. The SEM results in Figure 14 show that while there may have been CONs suspended in the water, most of the suspended particles appeared to have the particulate rather than nanosheet morphology.

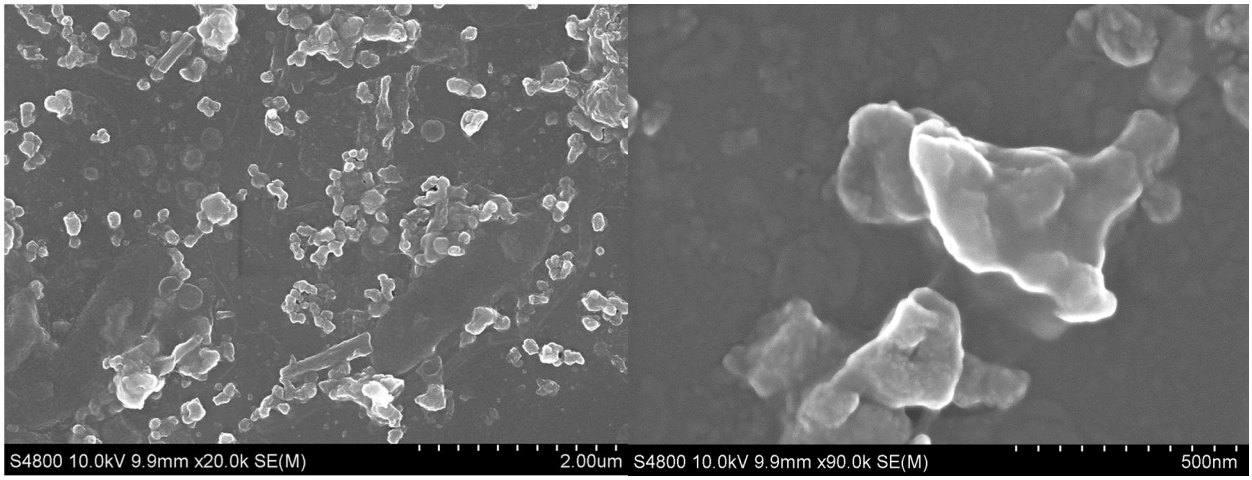

Figure 14: SEM of CON suspension

The confocal microscope images support these results and display the lack of uniformity among the particle sizes. Figure 15 shows the diversity in particle size, indicating inadequate methods of separating CONs from COF particulate. The figure also shows how spread out the particles are from each other, indicating a lack of density required to form an adequate membrane layer.

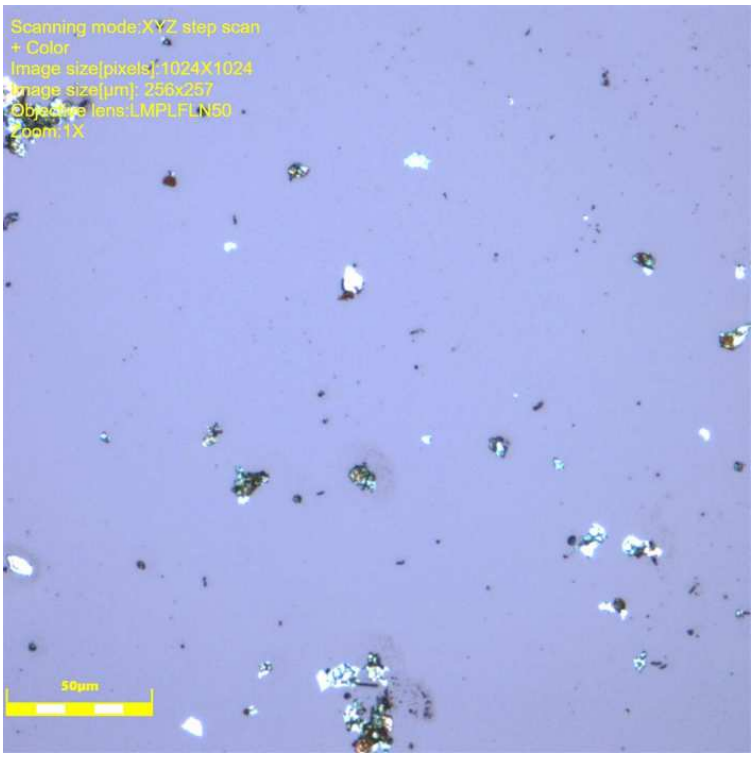

Figure 15: Confocal image of CON suspension at 50X magnification

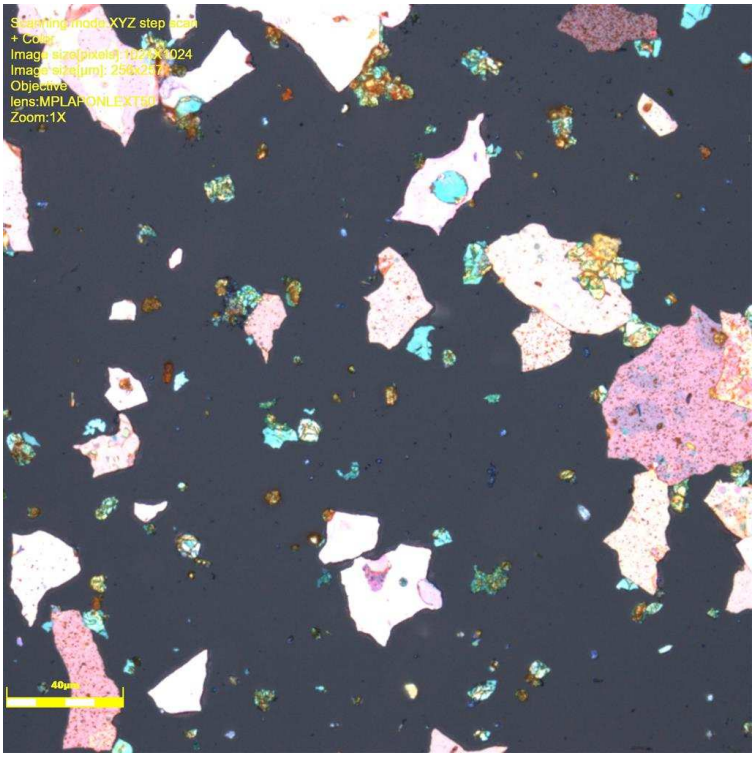

Figure 16: Confocal image of sonicated COF particulate without centrifugation at 50X magnification

While the CON suspensions proved to be inadequate at forming a selective membrane layer, a closer look at the particulate suspension after liquid sonication but before centrifugation revealed promising qualities of an unaltered COF thin film. Figure 16 shows the 50X magnification of the COF particulate suspension, which sheet-like COF fragments that appear flat enough to be used as a selective membrane layer. This indicates that the COF thin film polymerized at the beginning of the process could potentially serve as a membrane layer, if properly transferred to a porous support.

Table 1: Thickness measurements of COF particulate fragment

		Thickness[µm]
Count		5
Average		0.483
Max.		0.673
Min.		0.395
Range		0.279
σ		0.099

A step analysis feature of the confocal microscope software was used to measure the thickness of the COF particulate fragments. Table 1 shows the measured results of the thickness of one of the fragments with an average thickness of 483nm. This data further supported the possibility of using the COF thin film as a selective membrane layer.

Thin Film Membranes

All thin film membranes were prepared at the liquid-liquid interface and then transferred to a nylon support with a diameter of approximately 35mm and tested using a vacuum apparatus with a diameter of about 20mm. Using a smaller vacuum apparatus diameter allowed for specific portions of the membranes to be tested incase portions of the membrane had too many visible

defects. It also made it possible to more accurately calculate the permeance of the membranes by increasing the time it takes for a given volume to pass through. Each membrane was tested with 20mL of a standard 50 ppm Congo Red dye solution using the smaller vacuum apparatus. The time it took for the 20mL to pass through the membrane was used to calculate the permeance in $\frac{L}{bar*m^2*hr}$ and the collected permeate was analyzed using UV-Vis spectroscopy to calculate the dye rejection rate. Characterization of Tp, Pa, and TpPa-1 thin film was done using Fourier-transform infrared spectroscopy (FTIR). The FTIR data (Figure 17) for the Tp monomer shows peaks around 3,000cm^{-1} indicating a O-H bond, a peak at 1,650cm^{-1} indicating a C=O bond, and a peak around 1,450cm^{-1} indicating C-H bonding. For the Pa monomer, there is a peak around 1,620cm^{-1} indicating C=C bond, a peak near 1,500cm^{-1} indicating C-H bonding, and a peak near 1,250cm^{-1} indicating a C-N bond. For the TpPa-1, there is a peak at 1,580cm^{-1} indicating the presence of C=C and N-H bonding, a peak at 1,450cm^{-1} indicating C-H bonding, and a peak around 1,250cm^{-1} indicating C-N bonding. The loss of the O-H and C=O peaks in the TpPa-1trend indicate a successful polymerization between the Tp and Pa monomers. This data helps prove that the created thin film is TpPa-1. A confocal microscope was used to analyze the TpPa-1 thin films synthesized under each condition.

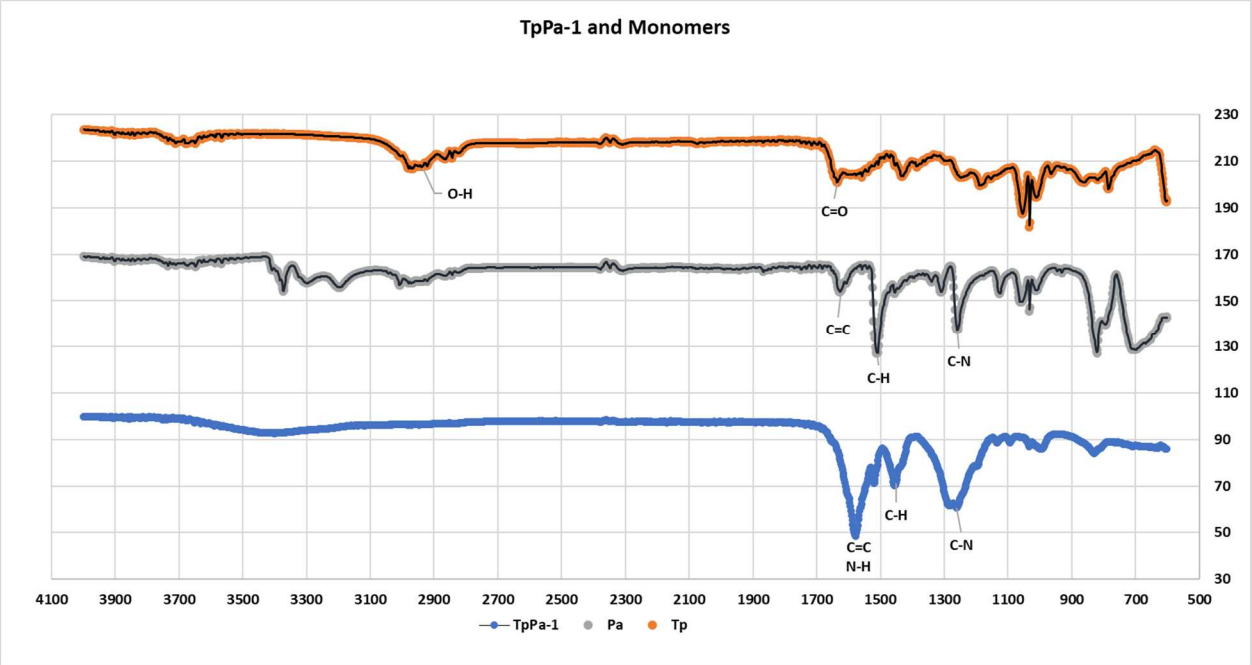

Figure 17: FTIR data for Tp monomer, Pa monomer, and TpPa-1 thin film

0.005% Thin Film

a) b)

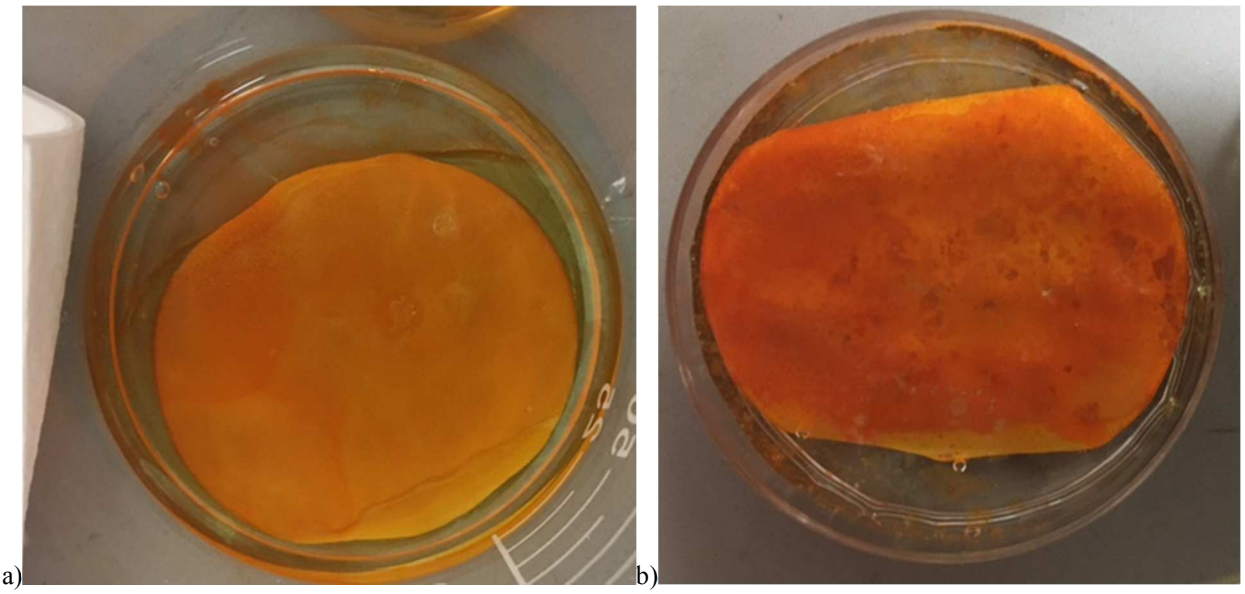

Figure 18: a) 0.005% TpPa-1 thin film on a nylon support before and b) after performing a secondary IP on the film.

The films created using 0.005% monomer concentrations and 72 hours of polymerization time seemed to have more flexibility than the films with higher monomer concentrations. This was evident by visually observing the cracks formed in the thin film while removing the liquid layers from the beaker with a pipette at the end of the polymerization. The 0.005% thin film seemed to move without cracking as much as the 0.01% and 0.02% thin films did and therefore produced better, more continuous membranes.

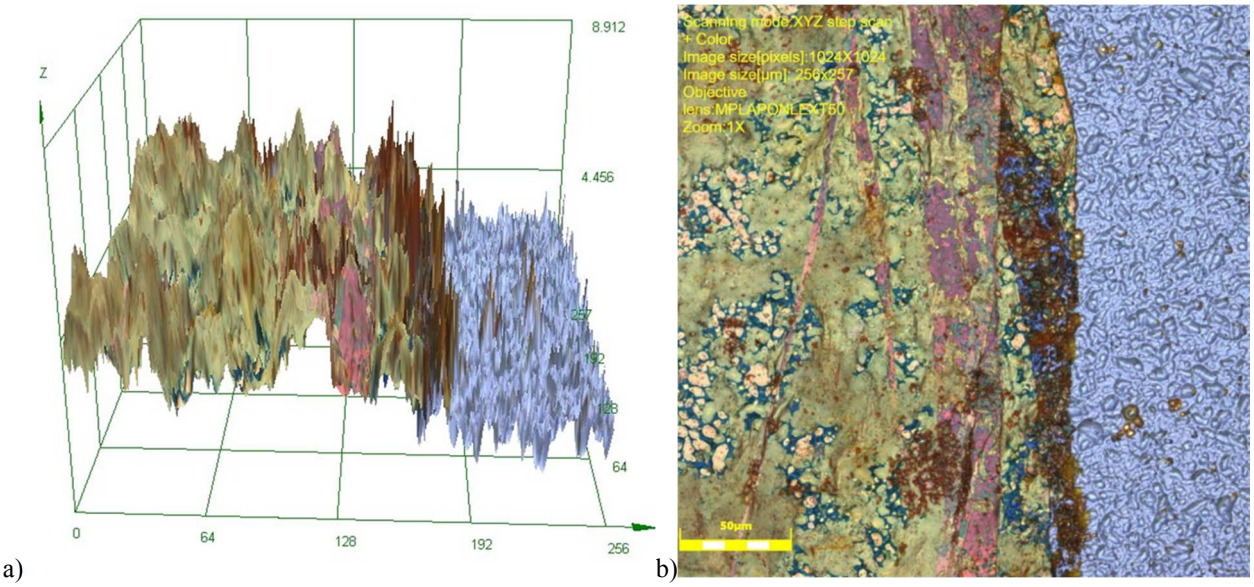

a) b)

Figure 19: a) 50x Confocal Microscope image of a 0.005% thin film in 3D and b) 2D.

Confocal images of the 0.005% thin film on a silicon wafer (figure 19a and b) were captured at 50x magnification. The roughness displayed in the 3D image is likely due to the film shriveling up as it dried on the wafer.

Table 2: Film thickness results for 50x confocal image of 0.005% thin film.

	Height[µm]
Average	**0.517**
Max.	**0.694**
Min.	**0.257**
Range	**0.438**
σ	**0.165**

Table 2 shows the film thickness data taken from the 50x confocal microscope image of a 0.005% thin film that had not received a secondary IP. The heights were measured using a step analysis feature on the confocal image software, which allowed the difference in height between the surface of the glass slide and the surface of the film. The data points represent the thickness of the film, the data indicates an average thickness of 0.517µm.

0.01% Thin Film

a) 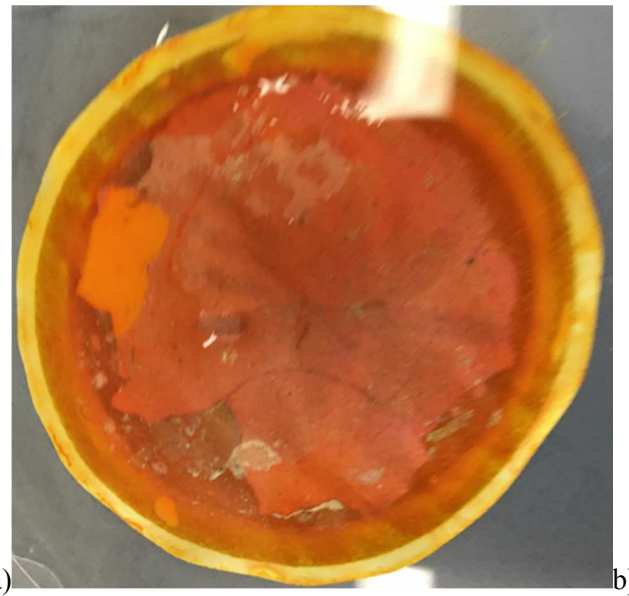 b) 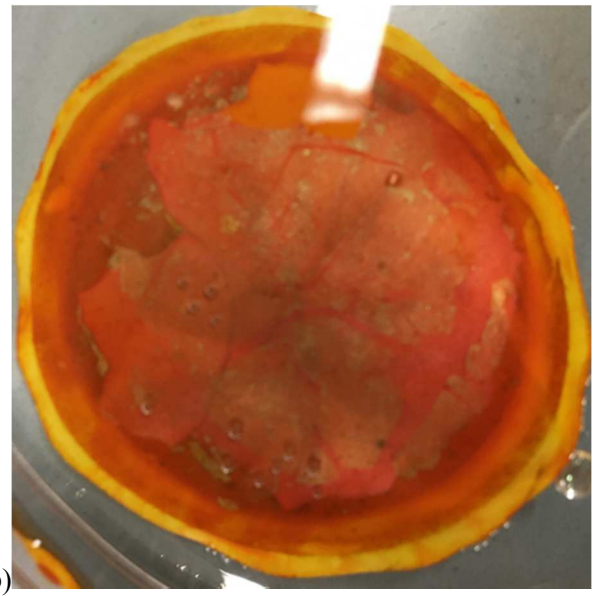

Figure 20: a) 0.01% TpPa-1 thin film on a nylon support before and b) after performing a secondary IP on the film.

The films created using 0.01% monomer concentrations and 72 hours of polymerization time seemed to have more issues with cracks forming than the 0.005% thin films. Large cracks formed more often and in some cases the film would snap down the middle when removing the liquid layers from the beaker, rendering the membrane useless

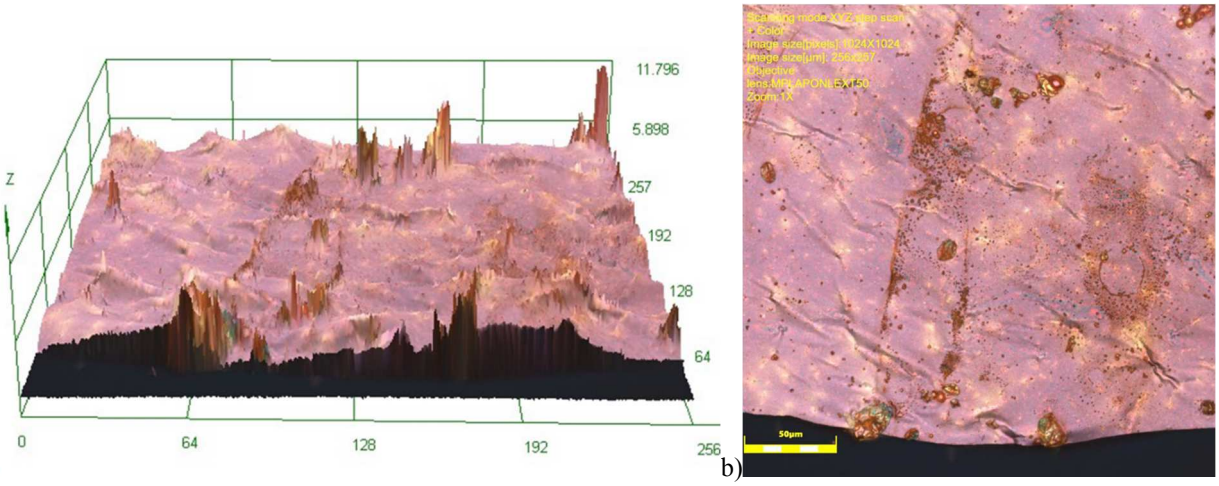

a) b)

Figure 21: a) 50x Confocal Microscope image of a 0.01% thin film in 3D and b) 2D.

Confocal images of the 0.01% thin film on a glass slide (figure 21a and b) were captured at 50x magnification. The surface appears to be smoother than the 0.005% thin film, which could potentially be a result of how the sample was prepared or the use of a glass slide instead of a silicon wafer. The surface does seem to be crinkled with some sharp peaks, which could be due to the effects of drying on the glass slide.

Table 3: Film thickness results for 50x confocal image of 0.01% thin film.

		Height[µm]
Average		**0.826**
Max.		**1.070**
Min.		**0.431**
Range		**0.639**
σ		**0.230**

Table 3 shows the film thickness data taken from the 50x confocal microscope image of a 0.01% thin film that had not received a secondary IP. The heights measured using the step analysis of feature of the confocal image software show an average thickness of about 0.826µm.

0.02% Thin Film

a)  b) 

Figure 22: a) 0.02% TpPa-1 thin film on a nylon support before and b) after performing a secondary IP on the film.

The films created using 0.02% monomer concentrations and 72 hours of polymerization time seemed to have the highest tendency to crack. With the thickest films produced, the 0.02% films were difficult to attach to the nylon support because the films would often snap while removing the liquid layers. This was likely due to the edges of the film sticking to the glass walls of the beaker and the lack of flexibility of the thicker film.

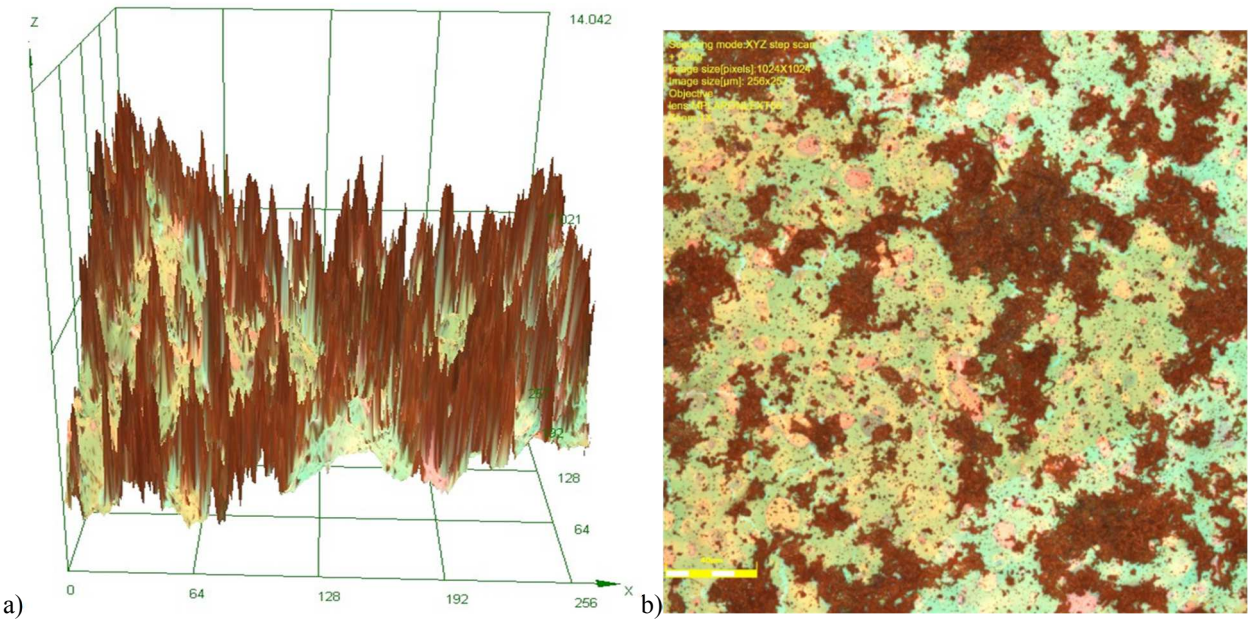

Figure 23: a) 50x Confocal Microscope image of a 0.02% thin film in 3D and b) 2D.

Confocal images of the 0.02% thin film on a silicon wafer (figure 23a and b) were captured at 50x magnification. The 3D image visually indicates that the 0.02% film had the roughest surface of the films analyzed. This is likely due to the thicker and less flexible structure of the film. It is also possible that the higher monomer concentrations produce a less even polymerization, producing a rougher thin film.

Table 4: Film thickness results for 50x confocal image of 0.02% thin film.

	Height[µm]
Average	**2.650**
Max.	**3.243**
Min.	**1.461**
Range	**1.783**
σ	**0.623**

Table 4 shows the film thickness data taken from the 50x confocal microscope image of a 0.02% thin film that had not received a secondary IP. The heights measured using the step analysis of feature of the confocal image software show an average thickness of about 2.650µm.

24 Hour 0.01% Thin Film

a) 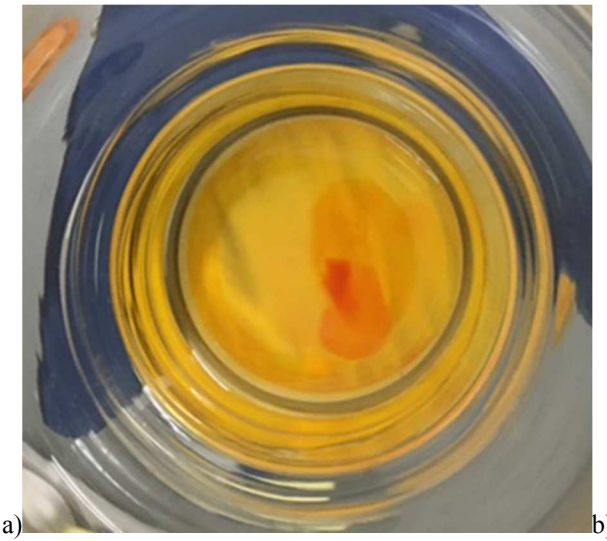 b) 

Figure 24: a) 0.01% TpPa-1 thin film synthesized for 24 hours on a nylon support before and b) after performing a secondary IP on the film.

The films created using 0.01% monomer concentrations and 24 hours of polymerization time seemed to be just as flexible as the 0.005% films. As the thinnest films, they were as easy to transfer to the nylon support without creating large, noticeable cracks in the film.

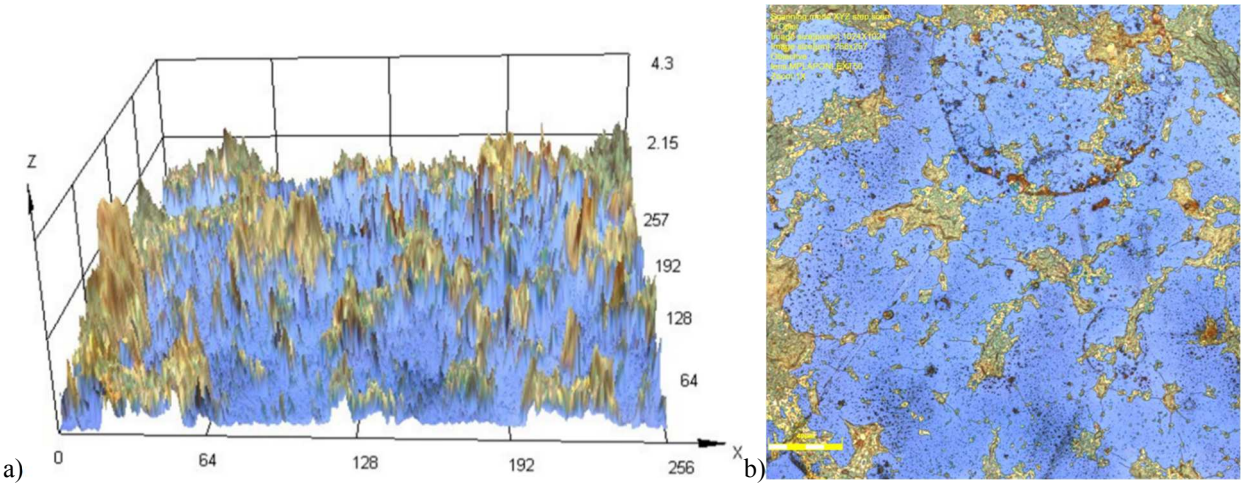

Figure 25: a) 50x Confocal Microscope image of a 0.01% thin film synthesized for 24 hours in 3D and b) 2D.

Confocal images of the 24-hour 0.01% thin film on a silicon wafer (figure 25a and b) were captured at 50x magnification. The blue and yellow appearance of the film under the microscope is likely a result of how light is reflected off the shiny surface of the film. The piece of film itself looked more yellow orange like the film seen in figure 24a before it was allowed to dry on a silicon wafer. Most of the peaks shown in figure 25a appear to yellow, which could indicate more concentrated areas of polymerization, making them thicker. This would be expected as the polymerization was not allowed the full 72 hours necessary to reach completion.

Table 5: Film thickness results for 50x confocal image of 0.01% thin film synthesized for 24 hours.

		Height[µm]
Average		**0.168**
Max.		**0.263**
Min.		**0.097**
Range		**0.166**
σ		**0.054**

Table 5 shows the film thickness data taken from the 50x confocal microscope image of a 0.01% thin film after only 24 hours of polymerization and had not received a secondary IP. The heights

measured using the step analysis of feature of the confocal image software show an average thickness of approximately 0.168µm.

48 Hour 0.01% Thin Film

a) 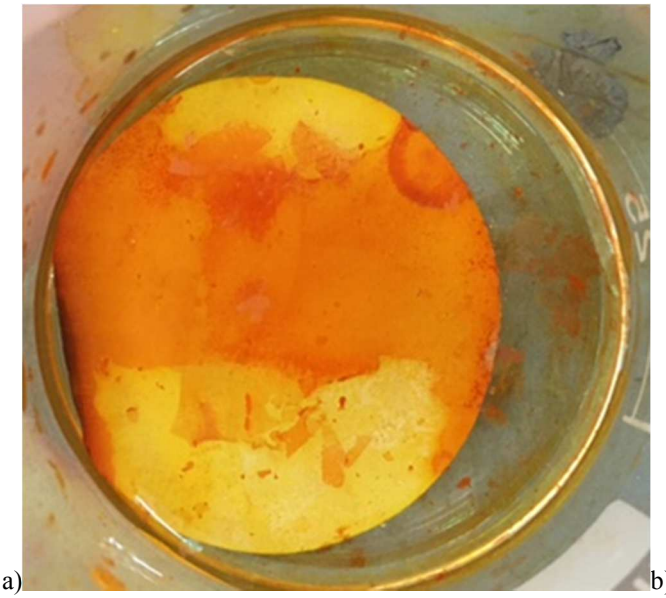 b) 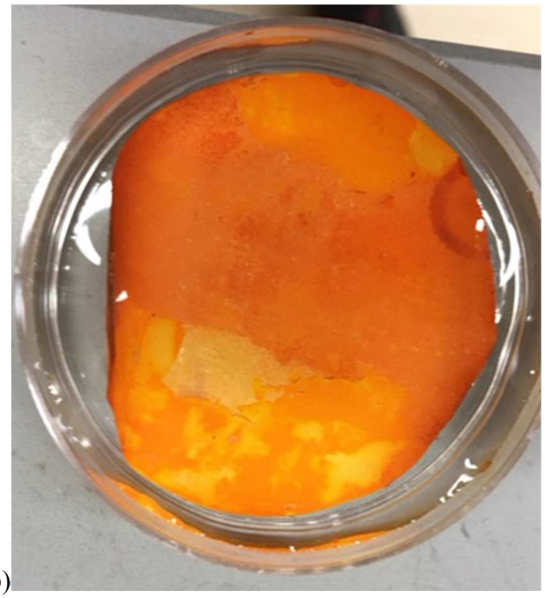

Figure 26: a) 0.01% TpPa-1 thin film synthesized for 48 hours on a nylon support before and b) after performing a secondary IP on the film.

The films created using 0.01% monomer concentrations and 48 hours of polymerization time seemed to be just as likely to form cracks as the 0.01% films polymerized for 72 hours. It appears the polymerization had enough time for the edges of the film to form a strong attachment to the glass walls of the beaker, but not enough time to form a flexible, continuous film.

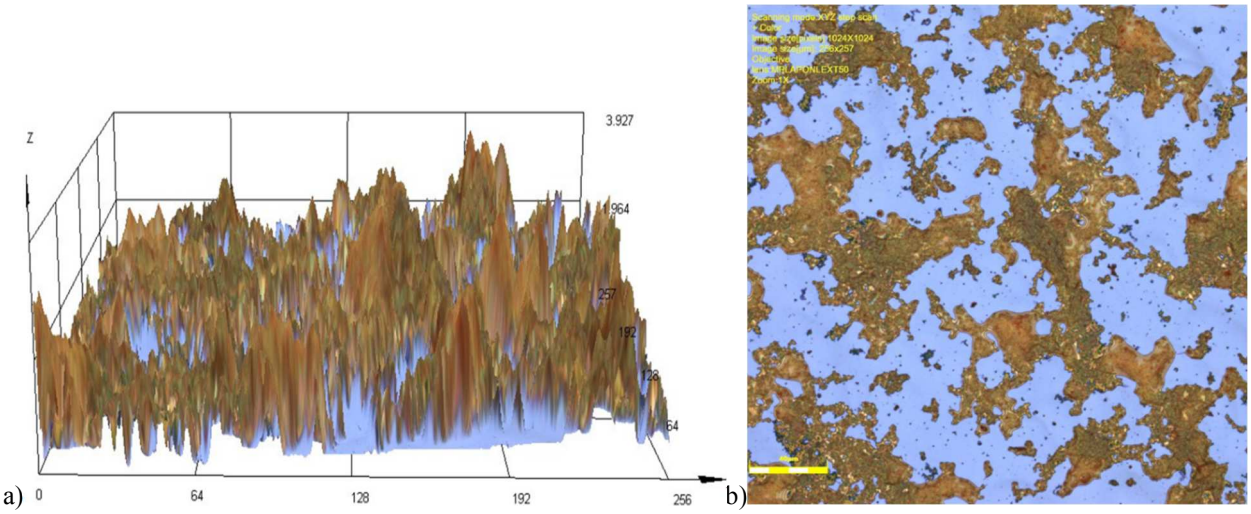

Figure 27: a) 50x Confocal Microscope image of a 0.01% thin film synthesized for 48 hours in 3D and b) 2D.

Confocal images of the 48-hour 0.01% thin film on a silicon wafer (figure 27a and b) were captured at 50x magnification. As with the 24-hour film, most of the peaks appear to be yellow. It can also be seen in figure 27a that the surface looks rougher and has a larger ratio of yellow to blue surface area than 24-hour film's surface. This supports the idea that the yellow peaks indicate areas of more concentrated polymerization occurring, since the increased polymerization time also led to more yellow peaks.

Table 6: Film thickness results for 50x confocal image of 0.01% thin film synthesized for 48 hours.

		Height[µm]
Average		**0.300**
Max.		**0.616**
Min.		**0.052**
Range		**0.564**
σ		**0.217**

Table 6 shows the film thickness data taken from the 50x confocal microscope image of a 0.01% thin film after only 48 hours of polymerization and had not received a secondary IP. The heights

measured using the step analysis of feature of the confocal image software show an average thickness of approximately 0.300µm.

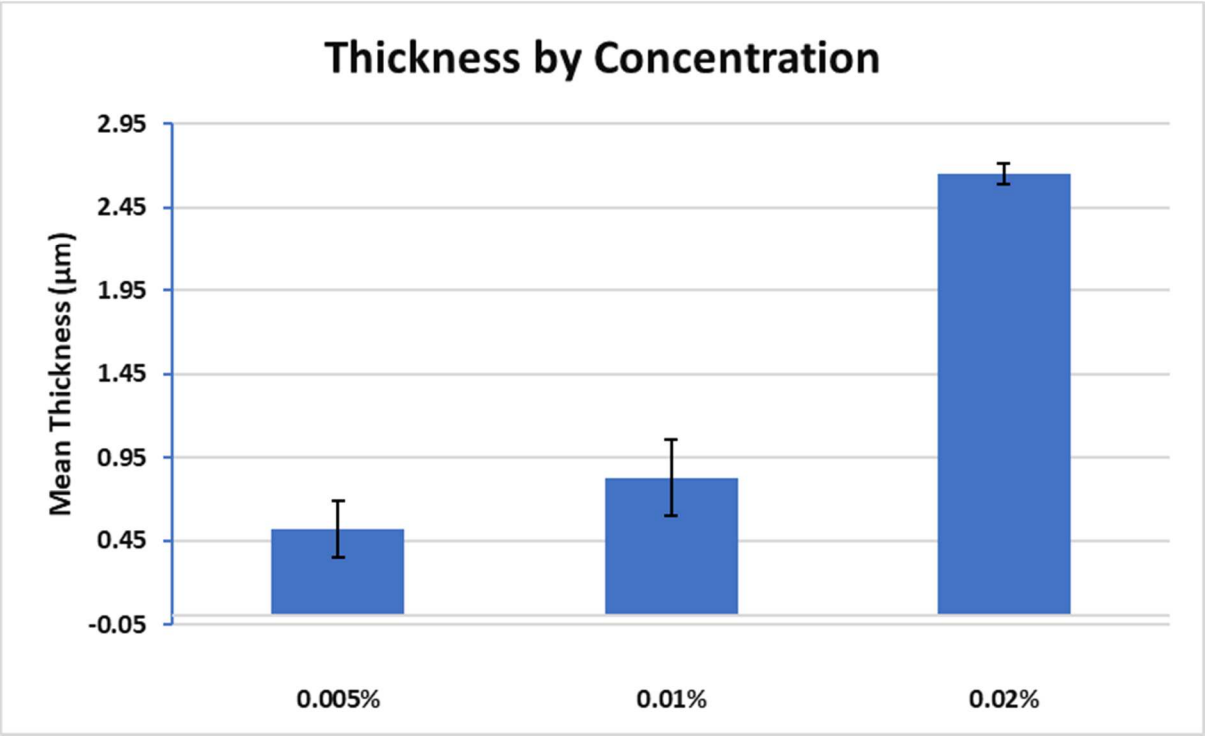

Figure 28: Bar graph of the measured average thicknesses of thin films by monomer concentrations, with standard deviations shown as error bars.

Figure 28 shows a side-by-side comparison of the thickness of films produced using varying monomer concentrations. As expected, increasing the monomer concentrations for the polymerization resulted in thicker films. A more linear relationship between monomer concentrations and film thickness was expected but more data points are needed to establish a more accurate trend.

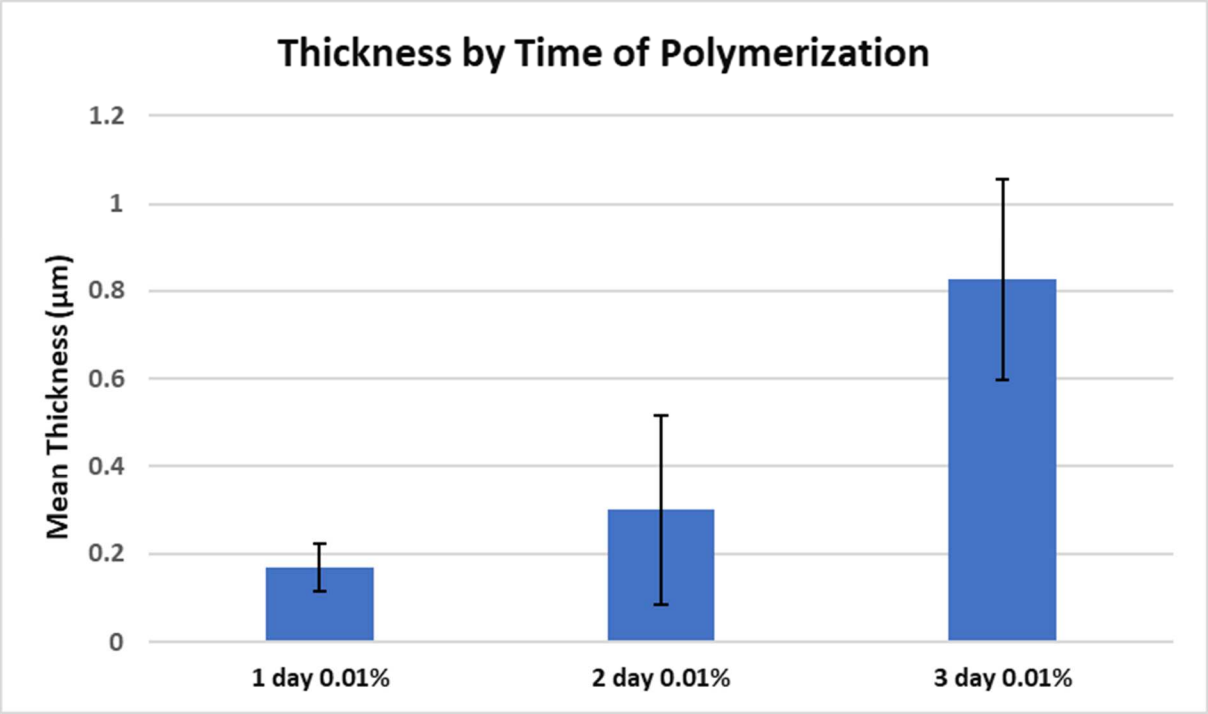

Figure 29: Bar graph of the measured average thicknesses of thin films by time of polymerization, with standard deviations shown as error bars

Figure 29 shows a side-by-side comparison of the thickness of films produced using varying polymerization times. As expected, decreasing the polymerization times resulted in thinner films. Again, a more linear relationship was expected, but not enough data was collected to establish a more accurate trend. Polymerization time appears to have the most impact on thickness, as the 1-day 0.01% film is less than half the thickness of the 0.005% thin film.

Membrane Performance

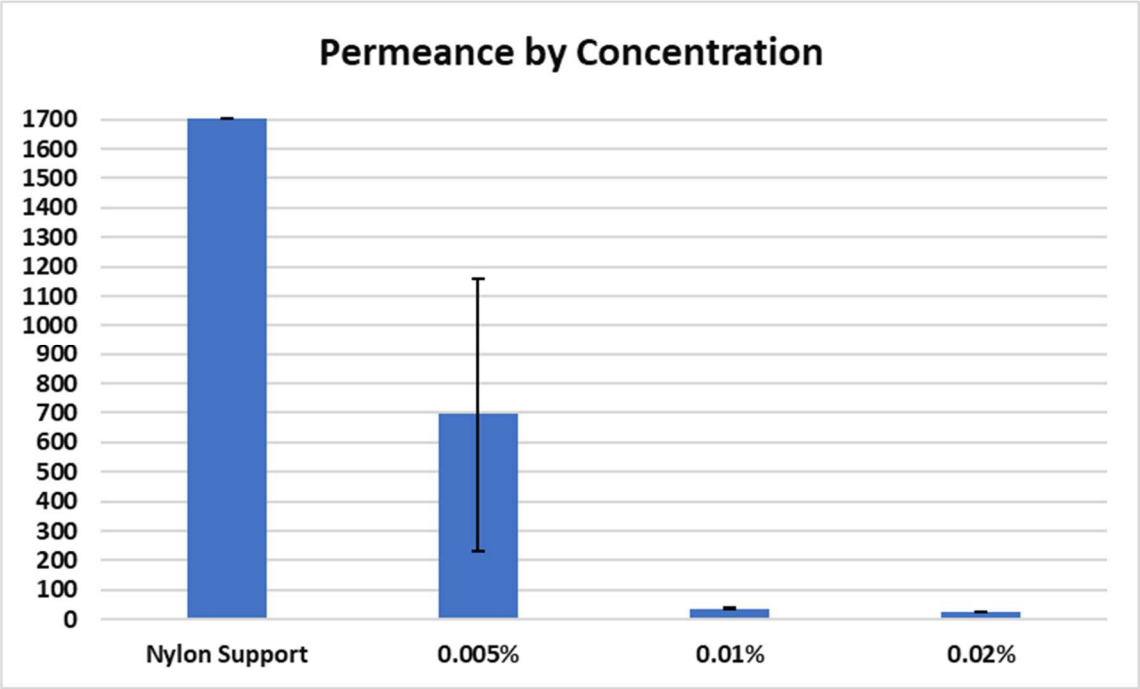

Figure 30: Measured average permeances of membranes in $\frac{L}{bar*m^2*hr}$ by monomer concentration.

Figure 30 shows the measured average permeances of Congo Red dye through membranes made using the various monomer concentrations in comparison with an unmodified nylon support. The large difference in measure permeance between the 0.005% films and the other films is likely a result of film defects. The thicker films produced with higher monomer concentrations tended to be less flexible and have more surface cracks. When testing the membranes, it appeared the dye would flow almost solely through the cracks on the membrane surface if they were present. Since the cracks had a very small surface area, the dye took more time to pass through them and therefore caused the membranes to have low permeances. When testing the membranes without major surface defects, the dye seemed to evenly pass through the tested surface area of the membrane, leading to higher measured permeances.

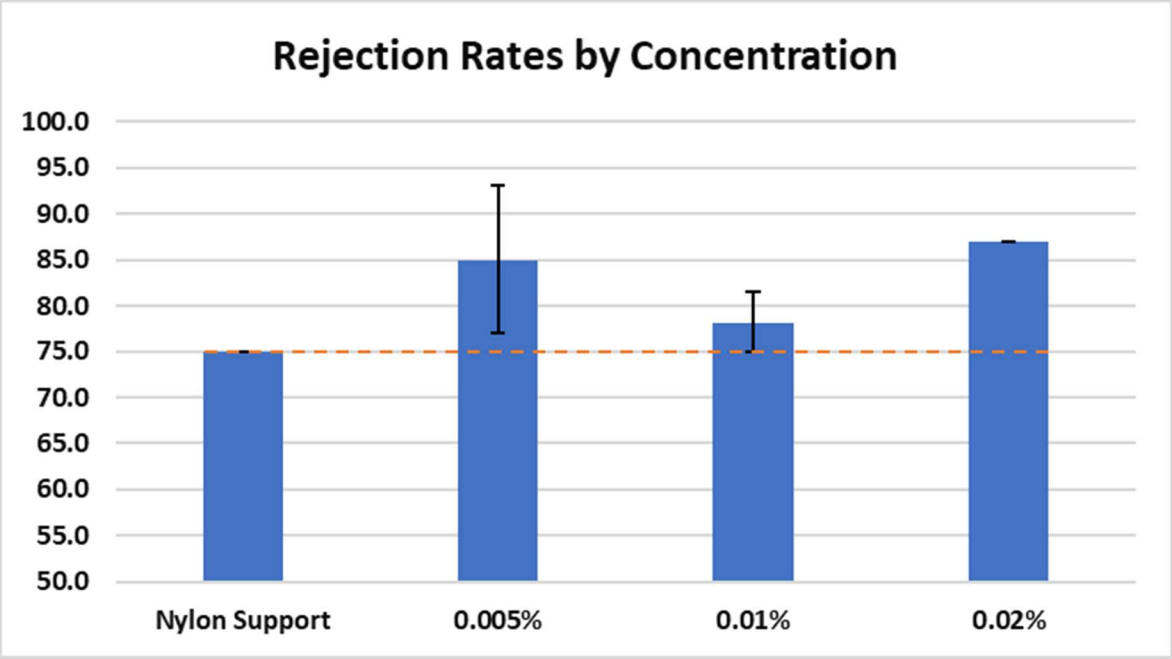

Figure 31: Measured average Congo Red dye rejection rates of membranes by monomer concentration.

Figure 31 shows the measured average rejection rates of Congo Red dye through membranes made using the various monomer concentrations in comparison with an unmodified nylon support. The nylon support alone was able to reject about 75% of the dye, which is not a result of size exclusion as the pores on the support were much larger than the dye molecules. The high rejection rate is more likely a result of same charge repulsion. Both the Congo Red dye and the nylon support are negatively charged and the repulsion of the two like charges seems to have prevented a high percentage of the dye molecules from pass through the support. The 0.005% membrane had rejection rates almost as high as the 0.02% membrane, while having much higher permeances. This is likely due to the 0.005% membranes having fewer defects in the thin film surface.

Table 7: Measured average membrane permeances and rejection rates by monomer concentration.

Membrane tested	Permeance (L/bar*m^2*hr)	Rejection Rate (%)
Nylon Support	1705	74.8
0.005%	696	85.0
0.01%	36	78.2
0.02%	26	87.0

Table 7 shows the permeance data and rejection rates for the membranes produced using different monomer concentrations with the performance of an untreated nylon support shown as well. While all permeances are higher than current commercial nanofiltration membranes (1-10 $\frac{L}{bar*m^2*hr}$), there is a non-linear yet clear trend of lower monomer concentrations having higher permeances. This makes sense as figure 28 shows that lower monomer concentrations produce thinner films. The 0.005% thin films produced membranes with similar rejection rates to the 0.02% thin films, but with a much higher permeance, and 0.01% thin films had the lowest rejection rates.

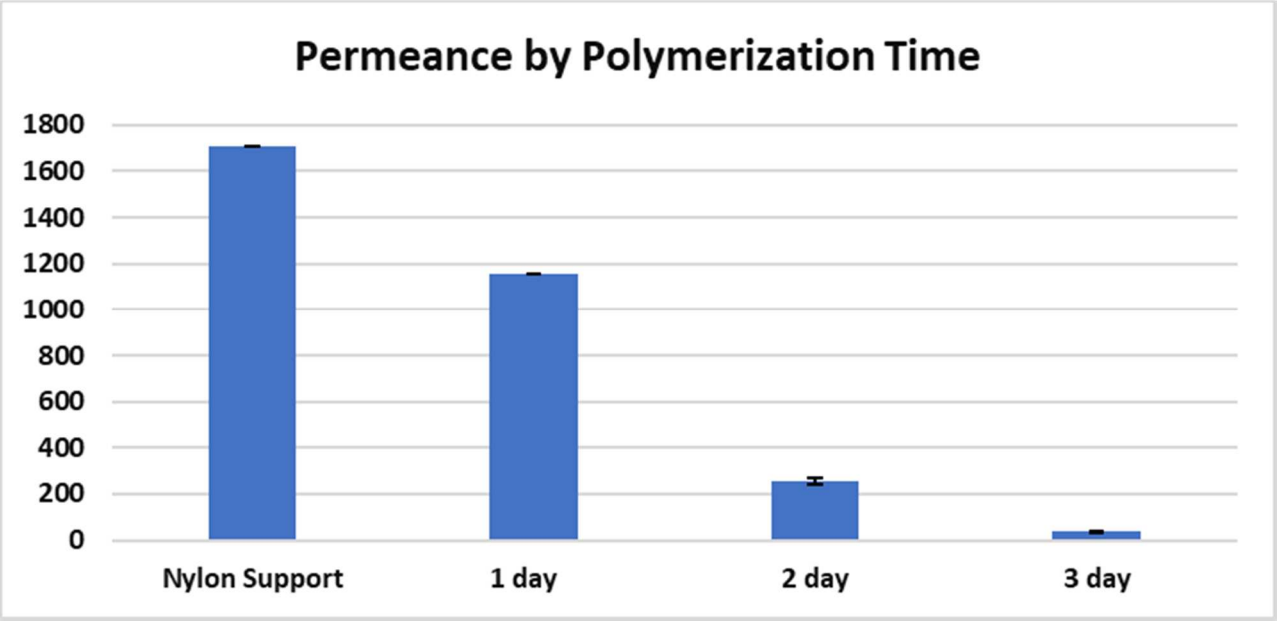

Figure 32: Measured average permeances of membranes in $\frac{L}{bar*m^2*hr}$ by polymerization time.

Figure 32 shows the measured average permeances of Congo Red dye through membranes made using the various polymerization times with 0.01% monomer concentrations in comparison with an unmodified nylon support. This data appears closer to the expected linear trend than the other graphs, with the 24-hour film having the highest permeance, and the permeance decreasing with increasing polymerization time. The 24 and 48-hour films appeared to have more flexibility and significantly fewer defects than all the films polymerized for 72 hours.

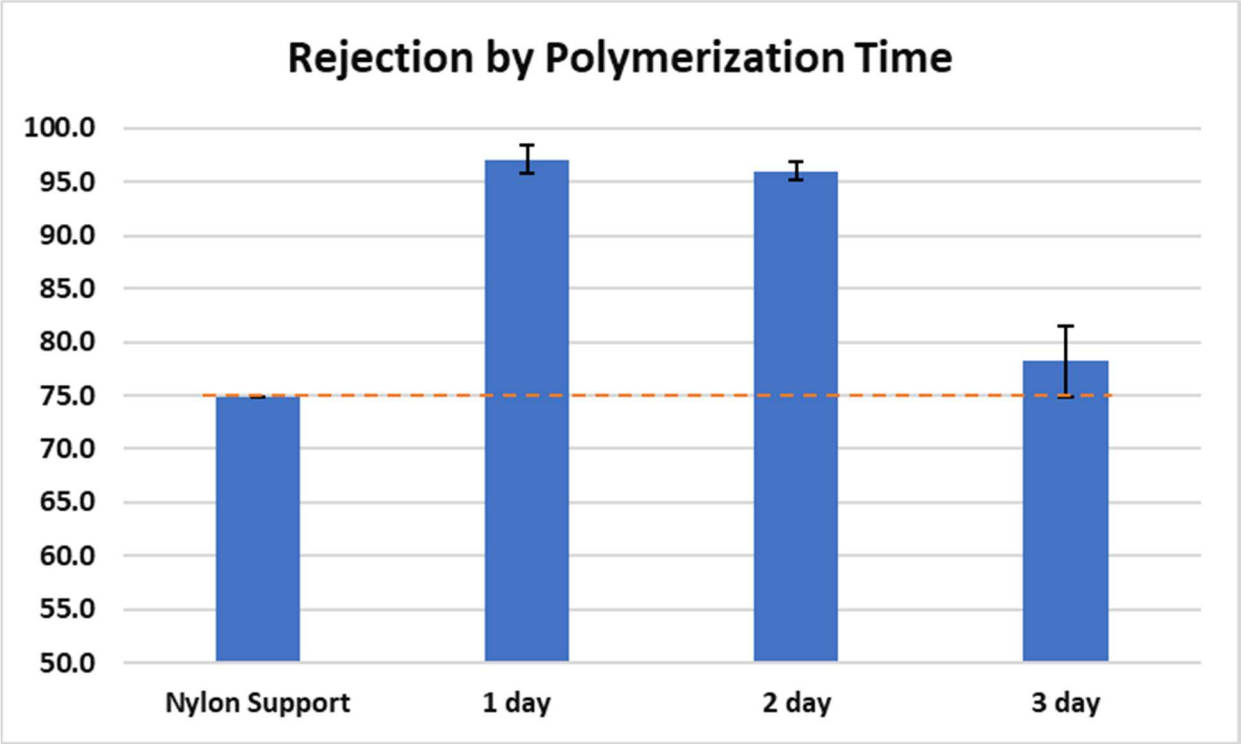

Figure 33: Measured average Congo Red dye rejection rates of membranes by polymerization time.

Figure 33 shows the measured average rejection rates of Congo Red dye through membranes made using the various polymerization times with 0.01% monomer concentrations in comparison with an unmodified nylon support. This graph shows a clear improvement in membrane performance by decreasing polymerization time. Not only did the 24 and 48-hour membranes

have much higher permeances, but they also had the highest rejection rates, over 95% for both. This displays the value in producing a more flexible defect free thin film layer when fabricating a membrane.

Table 8: Measured average membrane permeances and rejection rates by polymerization time.

Membrane tested	Permeance (L/bar*m^2*hr)	Rejection
Nylon Support	1705	74.8
1 day	1159	97.1
2 day	253	96.0
3 day	36	78.2

Table 8 shows the permeance data and rejection rates for the membranes produced using different polymerization times with the performance of an untreated nylon support shown as well. The permeances of all tested membranes were higher than $10\frac{L}{bar*m^2*hr}$, with the 2-day membranes being an order of magnitude higher, and the 1-day membranes being 2 orders of magnitude higher. This data follows the trend of thinner films producing membranes with higher permeances. This data also suggests that thinner films have better integrity and fewer defects and therefore higher rejection rates, as the 1 and 2-day thin films produced membranes with rejection rates above 95%.

Conclusion

The COF thin films' susceptibility to cracking while removing the liquid layers from the beakers made it difficult to produce quality membranes. With the data collected, it is clear the thin film thickness can be controlled and tuned by adjusting the monomer concentration and to a degree, adjusting the polymerization time. Allowing the thin film do polymerize 24 hours, as opposed to

the full length of 72 hours, produced thin films performed better than all other films in permeance and rejection rates. This high performance is likely due to the film's superior flexibility, high integrity, and much lower thickness.

The 48 hour thin films also produced membranes with high permeance in comparison to commercial NF membranes, while maintaining the second highest rejection rates at approximately 96%. With the 0.005% monomer concentration thin films producing the second highest performing membranes in terms of permeance and almost third highest rejection rates (just below the 0.02% rejection rates), evidence suggests thinner films produce membranes with higher permeance without sacrificing rejection rates.

While higher rejection rates coupled with higher permeances seems counterintuitive, this data suggests that thicker films are more prone to defects. Visual inspection of the membranes with low permeance and low rejection rates suggested that the dye would solely pass-through small defects, leaving small, dark marks on the membrane. The lack of flow through the other parts of the membrane without defects could be a result of COF layers stacked on top of each other in a way that eclipses the 2D pores to the point of being too small for water molecules to pass through.

Future Work

There is still plenty of room for improvement for fine-tuning the TpPa-1 thin film membranes. Decreasing the film thickness seems to keep on improving the permeance and rejection rate of the membrane. More adjustments can be made to scale down the monomer concentrations and polymerization time can be further analyzed. Other factors such as the secondary IP

concentration and quantity could also be fine-tuned to improve membrane performance. Perhaps most importantly a more delicate and less human-error prone method should be explored for the attachment of the COF thin film to the support layer. Additionally, there is plenty of analysis left to be done on the thin film membranes, including molecular weight cutoff and x-ray diffraction analysis.

References

1. S. Yuan, X. Li, J. Zhu, G. Zhang, P. Van Puyvelde and B. Van der Bruggen. *Chem. Soc. Rev*., **2019**, *48*, 2665
2. A. P. Cote, A. I. Benin, N. W. Ockwig, M. O'keeffe, A. J. Matzgerand O. M. Yaghi,Science, **2005**, *310*, 1166–1170.
3. A. Nagai, Z. Guo, X. Feng, S. Jin, X. Chen, X. Ding and D. Jiang,Nat. Commun., **2011**, *2*, 536
4. The World health report 2002 – reducing risks, promoting healthy life. Geneva, World Health Organization , **2002**
5. Er Bei, Xiaomei Wu, Yu Qiu, Chao Chen, and Xiaojian Zhang *Accounts of Chemical Research* **2019** *52* (4), 867-875
6. E. R. Gilliland *Industrial & Engineering Chemistry* **1955** *47* (12), 2410-2422
7. W. J. Koros, Y. H. Ma and T. Shimidzu. *Pure & Appl. Chem*., **1996**, *68* (7), 1479-1489
8. Audinos, R. and P. Isoard, eds., *Glossaire des termes techniques des procedes a membranes*, France: Societe Francaise de Filtration, **1986**
9. Glossary of Atmospheric chemistry Terms, compiled by Jack G. Calvert, Applied Chemistry Division, Commission on Atmospheric Chemistry, IUPAC, **1990**
10. M. Porter *Handbook of Industrial Membrane Technology*, Park Ridge, NJ: Noyes Publications, **1990**
11. Quantities, Units and SyrnboZs in Physical Chemistry, I. M. Mills, et al., Blackwell Scientific, **1993**
12. Standard D1129-90, ASTM Committee on Water, Subcommittee on Membrane and Ion Exchange, D19.08, Vol. 11.01, April **1991**
13. Standard D5090, ASTM Committee on Water, Subcommittee on Membrane and Ion Exchange D19.080, Vol. 11.02, May **1991**
14. *Terminology for Electrodialysis*, prepared by Karl Hattenback, European Society of Membrane Science and Technology, issued November **1988**
15. *Terminology for Membrane Distillation*, prepared by A. C. M. Franken and S. Ripperger, University of Twente
16. *Terminology for Pressure Driven Membrane Operations*, prepared by Vassilis Gekas, European Society of Membrane Science and Technology, issued June **1986**
17. *Terminology in Pervaporation*, prepared by K. W. Boddeker, European Society of Membrane Science and Technology, issued November **1989**
18. P. H. Duong, V. A. Kuehl, B. Mastorovich, J. O. Hoberg, B. A. Parkinson and K. D. Li-Oakey, *J. Membr. Sci*., **2018**, *574*, 338–348.
19. R. Kumar, A.F. Ismail, *J. Appl. Polym. Sci*., **2015,** 132
20. J. Lee, W. Tan, J. An, C. Cuah, C. Tang, A. Fane, T. Chong *Journal of Membrane Science,* **2016,** *499,* 480-490
21. T. Uragami, *Science and Technology of Separation Membranes,* **2017,** *4,* 87-103
22. H. Zhang, Q. He, J. Luo, Y. Wan, and S. B. Darling *ACS Applied Materials & Interfaces* **2020** *12* (36), 39948-39966
23. R. Wang, X. Shi, A. Xiao, W. Zhou and Y. Wang, *J. Membr. Sci.*, **2018**, *566*, 197–204.
24. S. Kandambeth, B. P. Biswal, H. D. Chaudhari, K. C. Rout, S. H. Kunjattu, S. Mitra, S. Karak, A. Das, R. Mukherjee and U. K. Kharul, *Adv. Mater.*, **2017**, *29*, 1603945.

25. H. Wang, Z. Zeng, P. Xu, L. Li, G. Zeng, R. Xiao, Z. Tang, D. Huang, L. Tang and C. Lai, *Chem. Soc. Rev.*, **2019**, *48*, 488–516
26. S. Chandra , S. Kandambeth , B. P. Biswal , B. Lukose , S. M. Kunjir , M. Chaudhary , R. Babarao , T. Heine and R. Banerjee , *J. Am. Chem. Soc.*, **2013**, *135* , 17853 —17861
27. M. A. Khayum , S. Kandambeth , S. Mitra , S. B. Nair , A. Das , S. S. Nagane , R. Mukherjee and R. Banerjee , *Angew. Chem., Int. Ed.*, **2016**, *55* , 15604 —15608
28. Z. Kahveci , T. Islamoglu , G. A. Shar , R. Ding and H. M. El-Kaderi , *CrystEngComm*, **2013**, *15* , 1524 —1527
29. S. Mitra , S. Kandambeth , B. P. Biswal , M. A. Khayum , C. K. Choudhury , M. Mehta , G. Kaur , S. Banerjee , A. Prabhune , S. Verma , S. Roy , U. K. Kharu and R. Banerjee, *J. Am. Chem. Soc.*, **2016**, *138* , 2823 —2828
30. Y. Song, J. Fan, S. Wang, *Materials Chemistry Frontiers*. **2017,** *1* (6), 1028–1040
31. F. Zhang, J. Fan, S. Wang, *Angew.Chem. Int. Ed.* **2020**, *59*, 21840–21856
32. S. Karan, Z. Jiang, A. G. Livingston, *Science* **2015**, *348*,1347 –1351
33. E. L. Wittbecker, P.W. Morgan, *J. Polym. Sci.* **1959**, *40*, 289–297
34. X. G. Li, J. Li, Q. K. Meng, M. R. Huang, *J. Phys.Chem. B* **2009**, *113*, 9718 –9727.
35. MacDiarmid, A. G. *Angew. Chem., Int. Ed*. **2001**, *40*, 2581
36. L. Brunsveld, B. J. B. Folmer, E.W.Meijer, R. P. Sijbesma, *Chem. Rev*. **2001**, *101*, 4071 – 4098
37. T. Aida, E. W. Meijer, S. I. Stupp, *Science* **2012**, *335*, 813 –817
38. M. Burnworth, L. Tang, J. R. Kumpfer, A. J. Duncan ,F. L. Beyer, G. L. Fiore, S. J. Rowan, C. Weder, *Nature* **2011**, *472*, 334 –337
39. T. F. A. de Greef, E. W. Meijer, *Nature* **2008**, *453*, 171 –173
40. K.Biradha, A. Ramanan, J. J. Vittal, *Cryst. Growth Des*. **2009**, *9*, 2969 –2970.
41. O. M. Yaghi, M. O'Keeffe, N. W. Ockwig, H. K. Chae, M. Eddaoudi, J. Kim*, Nature* **2003**, *423*, 705 –714.
42. Yang Z, Zhou Y, Feng Z, Rui X, Zhang T, Zhang Z. *Polymers* **2019**, *11,* (8) 1252.
43. Z. Joseph Parkerson, T. Le, P. Das, S. N. Mahmoodi, and M. R. Esfahani, *ACS ES&T Water* **2021** *1* (2), 430-439
44. G. Li, K. Zhang, and T. Tsuru, *ACS Applied Materials & Interfaces* **2017** *9* (10), 8433-8436
45. A. Xiao, Z. Zhang, X. Shi, and Y. Wang, *ACS Applied Materials & Interfaces* **2019** *11* (47), 44783-44791
46. R. Shevate and D. L. Shaffer, *ACS Nano* **2022** *16* (2), 2407-2418